TURBOJET-RAMJET PROPULSION SYSTEM FOR ALL-BODY HYPERSONIC AIRCRAFT

by Mark H. Waters

Office of Advanced Research and Technology
Mission Analysis Division
Moffett Field, Calif. 94035

NATIONAL AERONAUTICS AND SPACE ADMINISTRATION • WASHINGTON, D. C. • JANUARY 1971

1. Report No.	2. Government Accession No.	3. Recipient's Catalog No.
NASA TN D-5993		

4. Title and Subtitle	5. Report Date
TURBOJET–RAMJET PROPULSION SYSTEM FOR ALL–BODY HYPERSONIC AIRCRAFT	January 1971
	6. Performing Organization Code

7. Author(s)	8. Performing Organization Report No.
Mark H. Waters	A-3668
	10. Work Unit No.
9. Performing Organization Name and Address	789–50–01–01–15
Office of Advanced Research and Technology Mission Analysis Division Moffett Field, Calif. 94035	11. Contract or Grant No.
	13. Type of Report and Period Covered
12. Sponsoring Agency Name and Address	Technical Note
National Aeronautics and Space Administration Washington, D.C. 20546	14. Sponsoring Agency Code

15. Supplementary Notes

16. Abstract

The characteristics of a parallel, over-and-under, turbojet-ramjet propulsion system installed on an all-body Mach number 6 hypersonic aircraft are estimated, and the effect of variations in propulsion system parameters on payload and on problems of installation are determined. Engine thrust and fuel flow requirements are evaluated throughout acceleration and cruise, and the effects on the weights and dimensions of the propulsion system, including both inlets and engines, are determined. A wraparound turboramjet is also evaluated and comparisons with the parallel turbojet-ramjet system are made.

17. Key Words (Suggested by Author(s))	18. Distribution Statement
Hypersonic air-breathing propulsion Propulsion system integration All-body hypersonic aircraft	Unclassified–Unlimited

19. Security Classif. (of this report)	20. Security Classif. (of this page)	21. No. of Pages	22. Price*
Unclassified	Unclassified	55	$3.00

*For sale by the National Technical Information Service, Springfield, Virginia 22151

SYMBOLS

A	area, ft^2
A_c	cowl capture area, ft^2
A_{cwl}	cowl surface area, ft^2
$A_{D_{RJ}}$	ramjet duct area, ft^2
A_e	stream-tube area of engine inlet airflow, ft^2
A_{ex}	stream-tube area at the nozzle exit, ft^2
A_{spill}	spillage flow stream tube area (defined in fig. 40), ft^2
A_T	nozzle throat area, ft^2
C_f	compressible local skin-friction coefficient
C_{f_i}	incompressible local skin-friction coefficient
$C_{p_{M_l}}$	pressure coefficient at local Mach number M_l
$C_{p_{1.0}}$	pressure coefficient at Mach number 1.0
C_T	gross thrust coefficient
D_{cwl}	cowl drag, lb
D_R	ram drag, lb
D_{spill}	drag due to spillage, lb
$\frac{f}{a}$	fuel to air ratio
F_C	factor defined by equation (C4)
F_D	net propulsive thrust, lb
F_g	gross thrust, lb
F_L	net propulsive lift thrust, lb
F_R	factor define by equation (C5)

g	acceleration of gravity, 32.17 ft/sec^2
H_{cwl}	height of the cowl
K_L	length factor (see eq. (B2))
l	length of boundary-layer buildup, ft
L_{cwl}	cowl lift, lb
L_{RJ}	ramjet length, ft
L_{spill}	lift due to spillage, lb
M	Mach number
M_l	local Mach number
n	constant
p_b	static pressure on the vehicle aft surface, lb/ft^2
p_{cwl}	static pressure on cowl surface, lb/ft^2
p_{ex}	static pressure at the nozzle exit plane, lb/ft^2
p_l	local static pressure, lb/ft^2
p_s	static pressure behind first inlet shock, lb/ft^2.
p_T	total pressure, lb/ft^2
p_{T_N}	nozzle total pressure, lb/ft^2
p_{T_1}	total pressure ahead of the inlet, lb/ft^2
p_0	free-stream static pressure, lb/ft^2
p_1	static pressure behind vehicle bow shock, lb/ft^2
Q_l	local dynamic pressure, lb/ft^2
Q_1	dynamic pressure behind vehicle bow shock, lb/ft^2
R	gas constant for air, ft-lb/lb-°R
R_l	Reynolds number

T	static temperature, °R
T_T	total temperature, °R
T_{T_2}	engine face total temperature, °R
u	local boundary-layer velocity, ft/sec
U	free-stream velocity, ft/sec
V_1	air velocity at the engine inlet, ft/sec
W	cowl width
Wa	inlet airflow, lb/sec
W_{INL}	inlet weight, lb
W_{RJ}	ramjet weight, lb
y	normal distance from the wall, ft
α	vehicle angle of attack, deg (see fig. 38)
γ	ratio of specific heats
δ	cowl angle, first inlet ramp rangle, deg
δ^*	boundary-layer displacement thickness, ft
Δ_1	vehicle forebody half-angle at vehicle midsection, deg (see fig. 38)
Δ_b	vehicle aft half-angle at vehicle midsection, deg (see fig. 38)
θ	boundary-layer momentum thickness, ft
μ	air velocity, lb-sec/ft^2
ρ	air density, slugs

Subscripts

e	outer edge of the boundary layer
BL	boundary layer
INL	inlet

INV	inviscid
w	wall edge of the boundary layer
∞	free stream

Superscript

$( )'$	reference value derived from the reference temperature (eq. (C4))

TURBOJET–RAMJET PROPULSION SYSTEM FOR ALL–BODY HYPERSONIC AIRCRAFT

Mark H. Waters

Office of Advanced Research and Technology
Mission Analysis Division
Moffett Field, Calif. 94035

SUMMARY

The characteristics of a parallel, over-and-under, turbojet-ramjet propulsion system installed on an all-body hypersonic cruise aircraft are estimated, and the effects of variations in propulsion system parameters on payload and on problems of installation are determined. Engine thrust and fuel flow requirements are evaluated throughout acceleration and cruise, and their effects on weights and dimensions of the propulsion system, including both inlets and engines, are determined.

Cowl capture area and minimum turbojet engine size are determined by the thrust required to overcome the high transonic drag characteristic of the all-body vehicle, while the minimum size of the ramjet is determined by the thrust required at the Mach number for turbojet shutdown (between 3 and 4). Capture area, ramjet size, and the turbojet shutdown Mach number are all interrelated in terms of maximizing payload, but the payload sensitivity to these factors is relatively small. Since the capture area is sized at the transonic flight condition, the all-body vehicle does not cruise at the altitude for maximizing lift-drag ratio unless one or more of the following concepts are applied: the capture area is resized at cruise through the use of a variable area inlet design; the ramjets are throttled at cruise to decrease the fuel-air ratio; or the inlet is designed to spill some of the capture flow at cruise.

For a given thrust requirement, payload is increased as the number of engines is increased. The maximum number of engines is limited by the allowable propulsion system width. The payload sensitivity to the number of engines is slight; it is significant, however, for the assumptions made concerning the inlet pressure recovery, the forebody-inlet boundary layer buildup, and especially the expansion of the exhaust flow beneath the vehicle afterbody.

INTRODUCTION

The wing-body type of aircraft has been evaluated in previous studies (refs. 1 and 2) as a long-range, liquid-hydrogen-fueled, hypersonic transport. Currently, the all-body vehicle is being evaluated for this same hypersonic mission. This vehicle is attractive from the standpoint of good volumetric efficiency (i.e., high ratio of volume to surface area to accommodate the low-density hydrogen fuel.

For the all-body vehicles cruising at Mach numbers between 6 and 8, an attractive propulsion system consists of engines arranged as separate turbine engine-ramjet combinations along with a two-dimensional variable-geometry inlet. This propulsion system might not be as attractive for a wing-body transport which may favor integrated turboramjets with axisymmetric inlets. For cruise Mach numbers higher than 8, the scramjet appears to offer significant advantages over the ramjet (refs. 3 and 4).

The purpose of this study is to evaluate combinations of separate turbojets and ramjets arranged in parallel as propulsion systems for all-body hypersonic transports. In this arrangement, turbojets (ref. 5) are placed directly above an equal number of ramjets having rectangular cross sections. In this way, the vehicle afterbody surface may be used efficiently as an expansion surface for the ramjet exhaust gases. For comparison, a brief evaluation of a wraparound turboramjet propulsion system (ref. 6) for the all-body vehicle is included. The wraparound turboramjet is not considered to be an attractive engine for use with a two-dimensional inlet because of its large diameter. However, this engine-inlet combination was evaluated extensively in reference 7, and it is felt that an evaluation of the wraparound turboramjet in this study is warranted.

The present study was carried out with the aid of a computer program and is limited to a single mission: an all-body vehicle with a take-off gross weight of 500,000 lb cruising at a Mach number of 6 over the greater part of a typical 5,500 nautical mile flight trajectory. A complete synthesis of the aircraft system and its performance on the flight trajectory is carried out on the computer to determine payload as the figure of merit. First, a baseline propulsion system is defined and payload is determined for this baseline system. Then, the various assumptions made for this baseline system are perturbed to determine payload sensitivities.

SYSTEM CHARACTERISTICS

Mission

This study considers the single mission of a hypersonic transport with a take-off gross weight of 500,000 lb cruising at a Mach number of 6 over a 5,500 nautical mile flight trajectory. The computer program initially determines the size of the propulsion system, then calculates the performance during climb and acceleration, cruise, and finally unpowered descent. All variables of the aircraft system are synthesized by the computer program to arrive at payload as a figure of merit. This synthesis involves determining weights of the airframe and tank structure, tank insulation, propulsion system, fixed equipment, useful load, and fuel (which includes a 10-percent reserve).

Structural and insulation weights are computed in separate subroutines, and fixed equipment unit weights are taken primarily from the data in reference 2. Payload is determined by summing all the aircraft weights and subtracting from the take-off gross weight which is a fixed input. This is an iterative procedure since some of the fixed weight is related to the payload (e.g., passenger furnishing).

Vehicle Configuration

The all-body vehicle used for this study is shown in figure 1. The dimensions given are for a vehicle configuration that has not been optimized for maximum payload. The all-body shape consists of an elliptical cone forebody and an afterbody of elliptical cross section, which fairs to a straight-line trailing edge. The significant parameters that describe the shape of the all-body are the breakpoint ratio l_π/l, which is the ratio of the forebody length to the total vehicle length; the fatness ratio S_π/S, which is the ratio of the maximum cross-sectional area (which occurs at the breakpoint) to the vehicle planform area; the ellipse ratio a/b, which is the ratio of the major and minor axes of the forebody cross-section ellipse; and the leading-edge sweep, Λ. Any three of these parameters are sufficient to define uniquely the geometric shape. The method of computing the aerodynamics of the all-body is discussed in appendix A.

Propulsion System Configuration

The propulsion system of prime interest in this study is shown schematically in figure 2. Hydrogen-fueled turbojets are arranged in parallel above separate ramjets, which have rectangular cross sections. Performance of the turbojets is computed from the data given in reference 5, and a special subroutine was developed to compute the ramjet performance. Air for both engine types passes through a common, two-dimensional, variable-geometry inlet placed in the compression field of the vehicle forebody. These inlets are similar to the design outline in reference 7 and are representative of the current thinking for two-dimensional hypersonic inlet systems.

The local inlet mass-flow ratio versus local inlet Mach number plotted in figure 3 is somewhat arbitrary, although the transonic mass-flow ratio of 0.65 shown is about the current state of the art for two-dimensional supersonic inlets. The inlet operates shock-on-lip (local inlet mass-flow ratio of 1) at a local inlet Mach number of 3 and above. No provision is made in the inlet for diverting the boundary layer ahead of the inlet to bypass it around the propulsion system, or for bleeding the inlet flow along the ramps to control the boundary layer inside the inlet.

As indicated in figure 2, a door-type valve seals off the turbojet during high Mach number operation. An alternate shutter type valve that could be used for this purpose is also shown in figure 2. It may be necessary to seal off the turbojet exhaust ducting as well as the turbojet intake duct to achieve efficient expansion of the ramjet exhaust flow after turbojet shutdown.

Climb and acceleration to a flight Mach number of 0.8 is accomplished with only the turbojets operating because the ramjets produce little or no thrust below this Mach number. Both turbojets and ramjets operate from a flight Mach number of 0.8 to the point of turbojet shutdown. The Mach number at which the ramjets are turned on was chosen arbitrarily, but the Mach number at which the turbojets are shut down is subject to optimization with an upper limit at a flight Mach number of 4 or an inlet total temperature of 1600° R, whichever occurs first. These are the limits imposed on the engine in reference 5. After turbojet shutdown, the turbojet subsonic duct is sealed and the vehicle accelerates to cruise with ramjets only. When both power-plant types are operating, the performance of the ramjet is computed under the assumption that the ramjet exhaust expands only to the lower edge of the turbojet nozzle without mixing the two nozzle flows (point A in fig. 2). After turbojet shutdown, it is assumed that the ramjet exhaust can expand under the vehicle afterbody to the trailing edge. Performance is computed for the tubojets (and the turboramjets)

with the exhaust flow expanding only out to an area equal to the maximum cross-sectional area of the engine. Naturally, the flow will expand beneath the vehicle afterbody, but it is not known how efficient this expansion will be as the flow boundary changes from a circle to a plane. The methods used to account for propulsive forces are described in appendix A.

Trajectory

The flight trajectory plotted in figure 4 was held constant throughout the study. This trajectory is arbitrary in the sense that the transonic sonic-boom overpressure and the high Mach number maximum dynamic-pressure limits are chosen arbitrarily. In figure 4 the trajectory follows a constant sonic boom of 3-psf overpressure between Mach number 1.0 and 2.5. Note that the sonic boom characteristics of the all-body vehicle are recognized to be a more serious problem than for the wing-body configuration of reference 1 for two reasons: the cross-sectional area is high, and the volume is spread over a short length, which would lead to higher overpressures on the ground for a given shock wave intensity. Above Mach number 2.5 the trajectory follows a constant dynamic-pressure path of 1000 psf. A stoichiometric fuel-air ratio is normally maintained throughout the climb and cruise. However, results are also presented for lean ramjet fuel-air ratios during climb and acceleration or during cruise. During vehicle acceleration, it is assumed that for a given fuel-air ratio, angle of attack is changed continuously to balance lift with weight. During cruise, angle of attack and altitude are changed continuously to balance lift with weight and thrust with drag. When the capture area is resized for cruise, it is done so that the forces are balanced at a maximum vehicle lift-drag ratio.

DISCUSSION OF RESULTS

To demonstrate the effect of the propulsion system on vehicle performance, a baseline propulsion system is defined with somewhat optimistic characteristics and assumptions. The discussion is devoted mainly to the effect on payload when the characteristics and assumptions made for the baseline propulsion system are perturbed; but the procedures used in sizing the propulsion system and the consequent effects on the all-body vehicle are also discussed. Though some optimism may have been used in defining the propulsion system, the incremental effects of perturbing the characteristics and assumptions should be valid.

Baseline Propulsion System

The baseline propulsion system for this study is a combination of turbojets and ramjets arranged according to the following characteristics and assumptions:

1. Cowl capture area is constant throughout the flight.

2. The turbojet is shut down at a flight Mach number of 3.1.

3. The ratio of maximum ramjet throat area to cowl capture area is 0.5.

4. The ratio of maximum ramjet exit area to cowl capture area is 1.5 with turbojets operating and 4.5 with turbojets shut down (see fig. 2).

5. The ratio of ramjet duct area to maximum throat area is 1.15.

6. The turbulent boundary layer built up in the inlet flow from the vehicle nose to the inlet ramps is ingested into the engines.

7. The inlet pressure recovery corresponds to military specification MIL–E–5008B (January 1959), with a correction to the total pressure ahead of the inlet due to the boundary layer buildup on the forebody.

8. No provision is made for bleed or bypass flow in the inlet.

9. For a given thrust requirement, the number of engines is increased and individual engine size is decreased until the total width of the engines is 87 percent of the vehicle width at the beginning of the inlet ramps (this provides a minimum space for the landing gear).

10. The fuel-air ratio is stoichiometric during climb and cruise.

11. The ramjet combustion efficiency is 0.98.

12. The ramjet nozzle velocity coefficient for friction and divergence losses is 0.98.

13. The exhaust nozzle flow is in shifting equilibrium.

The cowl capture area of the baseline propulsion system is not specified and figure 5 shows the variation in vehicle payload as this area is varied. The ratios of payload to gross weight shown in figure 5(a) provide a basis for the relative payload curves plotted in figure 5(b) and throughout the rest of the paper. These payload levels are not intended to represent the maximum that can be achieved with the all-body configuration, since the vehicle shape parameters have not been varied in this study. However, the vehicle shape, as defined in figure 1, is representative of good all-body design. A cowl capture area of 150 ft^2 maximizes the payload as shown in figure 5 and this payload is designated as the nominal against which all subsequent payload variations will be compared.

The variations in engine, inlet, and fuel-weight fraction with cowl capture area are shown in figure 6, which breaks down the three main weight categories related directly to the propulsion system. It can be seen that engine weight has the greatest influence in establishing the capture area for maximum payload. (Appendix B outlines the methods used to predict propulsion system weights.) It is apparent from figures 5 and 6 that the effect of the capture area on propulsion system weights has a significant effect on payload.

Propulsion System Sizing

Inlet sizing– The propulsion system must be large enough to provide sufficient thrust for acceleration at any point in the trajectory. The critical point of minimum thrust minus drag (pinch

point) occurs transonically at a flight Mach number of about 1.2. An acceleration of 2 ft/sec^2 at a flight Mach number of 1.2 is used as a sizing criterion. A lower acceleration criterion leads to slightly higher payloads, but it is felt that 2 ft/sec^2 acceleration at the pinch point provides sufficient margin for hot-day operation.

Both turbojets and ramjets are operating between the flight Mach numbers of 0.8 and 3.1. Flow to the turbojets is governed by the airflow characteristic of the compressor, and the remainder of the inlet flow is passed through the ramjets. Since the ramjets are operating at a flight Mach number of 1.2, where the propulsion system is sized, there is an interplay between ramjet size and cowl capture area that affects the required turbojet size. Figure 7 shows how the captured air is apportioned between ramjets and turbojets for the baseline propulsion system. For a cowl capture area of 140 ft^2, the ramjet size is more than adequate to pass all the captured air not demanded by the turbojets. Note that the ramjet throat area, which varies to maintain a sonic throat velocity, is well below the maximum allowable. At a cowl capture area of 150 ft^2, the ramjets are just large enough to pass all the captured air not demanded by the turbojets. When the cowl capture area is increased to 160 ft^2, the ramjet throat is not large enough to pass all the captured air below a flight Mach number of 1.2, and additional air must be spilled around the inlet, resulting in some spillage drag.

At the point of turbojet shutdown, all the flow is ducted to the ramjets. For the three cowl capture areas of figure 7, the ramjets are too small to pass all the captured air at flight Mach numbers between 3.1 and 3.9, and again, some of this air must be spilled around the inlet. There is some question as to whether the inlet would unstart when the turbojets are shut down and a large portion of the captured air is spilled. In practice, the turbojets would not be shut down instantaneously, and hopefully a control system could be built into the inlet that would keep the inlet started. If this is not possible, then the alternative would be a bypass system that would dump the excess air from the subsonic diffuser to beneath the vehicle. At flight Mach numbers between 3 and 4, a bypass system probably would lead to higher drag penalties as well as an increase in weight. The logical solution is to run the turbojets to a higher Mach number so that the ramjets can handle a greater portion, if not all, of the captured inlet air after turbojet shutdown. This idea is developed further in the section on ramjet sizing. It is important to have a clear understanding of the factors involved in propulsion system sizing at the transonic pinch point, because the tradeoffs between payload, fuel weight, and propulsion system weight are dominated by the minimum acceleration requirements at this pinch point as will be reiterated in the following discussion.

Turbojet sizing– The amount of turbojet thrust required is dictated by the acceleration requirement at the transonic pinch point, as outlined in the previous section. The ramjet contributes thrust at the pinch point as long as the airflow captured by the cowl is greater than the turbojet demand. Therefore, ramjet size and cowl capture area affect the turbojet requirements. This effect for the baseline propulsion system is shown in figures 8(a), (b), and (c).

As capture area is decreased, the mass-flow ratio into the turbojet increases as shown in figure 8(a). This leaves less air to be burned in the ramjet, and the resulting loss in ramjet thrust must be made up with increased turbojet thrust to maintain the required acceleration of 2 ft/sec^2. This is demonstrated in figure 8(b), which shows the relative increase in the number of turbojets required as cowl capture area decreases, and in figure 8(c), which translates the increase in number of engines into an increase in the ratio of sea level static thrust to vehicle gross weight.

Thus, as cowl capture area is decreased, the inlet airflow supply is decreased, while paradoxically, the turbojet airflow requirement is increased. At a cowl capture area of 136 ft^2, the turbojet demand balances the inlet supply (fig. 8(a)), and no air passes through the ramjet at a Mach number of 1.2. Further reductions in cowl capture area are unreasonable, since the terminal shock-wave system of the inlet would be drawn downstream from its normal running position, leading to high total pressure losses through the terminal shock wave.

Although the optimum capture area is reasonably well defined, the total variation in payload shown in figure 5 is only 0.6 percent of the vehicle gross weight. More significant is the fact that payload drops rapidly as cowl capture area is decreased to the point where the inlet supply of air matches the turbojet demand at the pinch point. Thus, it is desirable to have some ramjet thrust transonically because even though the turbojets are much more efficient at these Mach numbers, they are much heavier than ramjets, and the high level of thrust is required only for a very short duration.

Ramjet sizing– The mass flow curves of figure 7 demonstrate the situation at the second pinch point – the Mach number at which the turbojet is shut down. At this point, all the inlet air is ducted to the ramjet, and for the capture areas shown, the ramjet nozzle is not big enough to pass all the flow. The remainder of the captured airflow either must be spilled around the cowl or dumped overboard ahead of the ramjets in a bypass system. As discussed previously, it is assumed in this study that the excess air can be spilled. The important factor at the second pinch point is whether the ramjets provide enough thrust for the vehicle to accelerate. Two approaches can be used to improve acceleration at this second pinch point: leave the turbojets on to a higher flight Mach number or use larger ramjets.

The effect of turbojet operation to higher Mach numbers on payload is shown in figure 9(a). There is a turbojet shutdown Mach number that maximizes payload as a result of minimizing the fuel consumption as shown in figure 9(b). The effect of the turbojet shutdown Mach number on acceleration is demonstrated in figure 9(c). Note that at turbojet shutdown, the acceleration jumps from the turbojet-plus-ramjet line to the ramjet-only line, which is a decrease from 15 to 2 ft/sec^2 in the case of the baseline systems (turbojet shutdown Mach number of 3.1). With regard to the problem caused by suddenly increasing the inlet spillage when the turbojets are shut down, figure 9(a) shows that there is very little decrease in the payload below the maximum as the turbojets are run to higher Mach numbers. Thus, as suggested earlier, the obvious solution to controlling the inlet shock system when the turbojets are shut down is to run the turbojets to a higher Mach number where there will be little or no change in the airflow through the inlet.

The effect of changing ramjet size on payload is shown in figure 10(a). The size of the ramjet is measured by the ratio of the maximum throat area to the cowl capture area. Payload is maximized by decreasing the size of the ramjets almost to the point of zero acceleration because of the decreasing weights of both the ramjet engines and the inlets, as shown in figure 10(b). The resulting effect on vehicle acceleration is shown in figure 10(c).

It is clear that the ramjet size and the turbojet shutdown Mach number are interrelated in the sense that for each ramjet size there is a different turbojet shutdown Mach number that will maximize the payload. This relationship is demonstrated in figure 11(a), which shows that maximum payload is obtained for a ramjet maximum throat area to cowl capture area ratio of approximately 0.3 and a turbojet shutdown Mach number of approximately 3.7. Basically,

figure 11(a) shows that a smaller ramjet can be used if the turbojet is run to higher Mach numbers. The minimum size of the ramjet at a given turbojet shutdown Mach number is dictated by the acceleration requirement at the second pinch point. This is demonstrated in figure 11(b) for acceleration levels between 0 and 10 ft/sec^2. However, the ramjet also plays a role in the turbojet sizing, and the ramjet size that maximizes payload is not necessarily the minimum allowable ramjet size at the second pinch point.

Vehicle Acceleration

The variation in vehicle acceleration with flight Mach number is demonstrated in figure 12. Acceleration is high, except at the transonic pinch point, and at a second pinch point which occurs when the turbojets are shut down. From the standpoint of passenger comfort, these acceleration levels are probably too high for a transport vehicle, in which case the engines would have to be throttled to maintain an acceptably low acceleration. Results are also shown on figure 12 for a throttled ramjet. Ramjet fuel-air ratio is arbitrarily reduced to a minimum of 0.02, but little effect is achieved until the turbojets are shut down. After turbojet shutdown, a maximum acceleration of approximately 10 ft/sec^2 is maintained with about a 2 percent loss in payload. It was not possible to present data for a throttled turbojet since the data in reference 5 are for a stoichiometric engine. However, throttling the turbojets would not decrease payload significantly.

Effect of Increasing Inlet Mass-Flow Ratio at a Mach Number of 1.2

The low acceleration at the transonic pinch point as shown in figure 12, is caused by the high transonic drag of the all-body vehicle. The thrust required to overcome this drag and to accelerate results in a relatively large turbojet size. A convenient measure of turbojet size is the ratio of the thrust at sea level static to the vehicle gross weight. This ratio for the baseline system (cowl capture area = 150 ft^2) is 1.17 as shown on figure 8. In contrast, for a typical winged-body hypersonic aircraft, this ratio may be as low as 0.5. To reduce the required turbojet thrust, it would seem reasonable to increase ramjet thrust as much as possible at the transonic pinch point. The fuel-air ratio in the ramjet is already stoichiometric. Thus, the only way to increase ramjet thrust is to increase the airflow into the ramjet by taking aboard the flow that is already being spilled. For a given cowl capture area, this can be done only by increasing the transonic mass-flow ratio of the inlet. This approach has the added benefit of reducing the inlet spillage drag. However, it is more difficult to design an inlet with high transonic mass-flow ratio that is also capable of operating with high performance over a wide range of Mach numbers.

An inlet schedule with a transonic mass-flow ratio of 0.8 is shown in figure 13, as well as the schedule for the baseline system. A larger throat in the inlet, which means increasing the vertical travel of the inlet ramp system, and a larger ramjet nozzle area are required to handle the increase in airflow over that for the baseline system at the transonic pinch point. Therefore, the optimum payload depends on the tradeoff between increased ramjet thrust, which reduces the weight of the turbojets, and the increased weight of the ramjets.

The sea-level static thrust to vehicle gross weight ratio and payload that result for an inlet with a transonic mass-flow ratio of 0.8 are shown in figures 14 and 15, respectively. The turbojet thrust to gross weight ratio decreases markedly as ramjet size is increased, but there is very little change in

the maximum payload obtained. This means that the tradeoff between ramjet thrust and ramjet weight in terms of maximum payload, is essentially balanced; that is, the decrease in turbojet weight and inlet spillage drag has been cancelled out by the longer and thus heavier inlet necessary to match the larger ramjet size and by the increased ramjet weight. This fact is demonstrated in figure 16, which shows increasing weight fractions of both the inlet and the engines as the size of the ramjets is increased. The engine weight fraction is the sum of both the ramjets and turbojets, and engine weights are increasing with the larger ramjet size even though the turbojet size is decreasing (as demonstrated by the sea-level static thrust to gross weight ratio in fig. 14). This means that a lighter weight ramjet could possibly reverse this trend and show payload increases with larger ramjets. The assumptions made for engine weights are discussed in appendix B.

Although no significant gains in payload are shown, the increase in transonic inlet mass-flow ratio does allow a larger ramjet and a smaller capture area without a penalty in payload. This eliminates the problem of low acceleration at the second pinch point, as demonstrated in figure 17 for ratios of the maximum ramjet throat area to cowl capture area up to 0.8. In other words, the high transonic mass-flow ratio has made it possible to achieve nearly maximum payload over a wider range of ramjet sizes, thereby making the acceleration at the second pinch point more selective without affecting payload.

Effect of Boundary Layer

For the baseline system computations, it is assumed that the turbulent boundary layer built up on the forebody of the vehicle from the vehicle bow to the inlet ramps is ingested into the inlet. Appendix C outlines the methods used to compute boundary layer displacement and momentum thicknesses along the vehicle forebody up to the beginning of the inlet ramps, and the resulting estimated loss in total pressure and decrease in the ram drag. The length of the boundary layer buildup for the baseline vehicle is approximately 120 ft, and if this boundary layer is ignored in performance calculations the effect is a 10-20 percent increase in the baseline payload as shown in figure 18. The ingestion of the boundary layer will also lead to added distortion of the inlet flow, but this should not be as much of a problem for the ramjet engines as it would be for the turbojets. During turbojet operation, and probably during ramjet operation, the ingestion of the boundary layer may be an important factor in the design of the inlet ducting.

It may be difficult to design a variable geometry inlet that will operate with the ingested boundary layer from the vehicle forebody because of inlet flow separation problems. If ingestion of the boundary layer is not feasible, bleed slots in the throat of the inlet and boundary-layer diverters ahead of the first ramp will be required to bypass the boundary layer around the propulsion system. These requirements were not evaluated in this study, but the weight of the hardware needed for the bypass ducting, the additional regenerative cooling requirements, and the drag of this ducting are the penalties that would have to be evaluated against the boundary-layer ingestion penalties.

Effect of Inlet Pressure Recovery

The baseline propulsion system uses the pressure recovery schedule of military specification MIL–E–5008B. This schedule applies to the reduction of total pressure from the beginning of the inlet ramps to the engine face. As discussed in the previous section, there is a correction to the total

pressure ahead of the inlet due to losses in the forebody boundary layer. A mass-averaged local Mach number is computed just ahead of the first inlet ramp based on a constant static pressure across the boundary layer, and this local Mach number is used in the pressure recovery schedule to determine the total pressure at the engine face. This schedule is probably optimistic for an inlet designed for minimum inlet ramp length and for ingestion of the forebody boundary layer. Figure 19 compares the payloads for various lower pressure recovery schedules with that for the baseline. A comparison of schedules 2 and 3 indicates the importance of keeping recovery high transonically where the propulsion system is being sized. A lesser gain is realized by keeping recovery high during the total acceleration, as can be seen from schedules 3 and 4. A comparison of schedules 1 and 4 shows the smallest loss in payload when high recovery is maintained throughout acceleration but not at cruise; a comparison of schedules 1 and 5 shows a relatively larger loss in payload for having low recovery throughout acceleration and high recovery during cruise only.

Methods of Cruising at or Near Maximum Lift-Drag Ratio

The baseline propulsion system has been defined to have a fixed capture area, which is sized at the transonic pinch point, and a stoichiometric ramjet fuel-air ratio throughout acceleration and cruise. With these requirements, it is impossible to cruise the all-body vehicle selected for this study at the altitude and angle of attack necessary for maximum lift-drag ratio. The inlet is oversized for cruise, and thus the vehicle must increase altitude to balance thrust and drag with a corresponding increase in angle of attack. The cruise angle of attack of the all-body vehicle with the baseline propulsion system is approximately 12°, whereas, its angle of attack for maximum lift-drag ratio is approximately 7°. This section discusses three methods of changing cruise altitude and angle of attack so as to cruise closer to the maximum lift-drag ratio of the aircraft.

Variable capture area– The baseline system capture area is sized at the transonic point, and this area is fixed throughout the flight. It would be desirable to have a variable capture area inlet, which would reduce the capture area at cruise and permit flight at the altitude that results in a maximum lift-to-drag ratio – provided the cowl drag and the necessary actuator and control weights for variable capture area are not excessive. Two approaches to varying the capture area by pivoting the cowl surface are analyzed. In the first, the capture area is sized transonically, and the cowl is pivoted inward to reduce the size for cruise, presenting a wedge surface at a positive angle of attack to the shock field flow. The resulting oblique shock raises the pressure on this surface, resulting in both a drag and a lift force. In the second approach, the capture area is sized for cruise, and the cowl is pivoted outward to increase the size transonically. This presents a wedge surface at negative angle of attack to the shock field flow. The flow expands around the corner of the cowl, resulting in a loss in lift and either a thrust or a drag force (depending on the amount of expansion).

The results for a reduced cowl capture area at cruise are shown in figure 20. The capture area during acceleration that maximizes payload is approximately 150 ft^2 with the cruise capture area reduced to about 65 percent of this value, or 97 ft^2. The drag of the cowl during cruise can be reduced by increasing the length of the pivoting cowl to reduce the cowl wedge angle. An optimum cowl length is obtained because of the tradeoff between increased weight of the actuators and controls with increased cowl length (see appendix B) and reduced drag. Figure 20 demonstrates that the problems of cowl drag and additional weight outbalance the advantage of resizing the capture area to cruise at maximum lift-drag ratio, and there is a significant loss in payload.

The results for an increased cowl capture area during acceleration are shown in figure 21. It has been assumed that the capture area is resized transonically and maintained at this size throughout the acceleration. The additional cowl drag results in zero acceleration at the second pinch point for capture areas less than 150 ft^2. Running the turbojets to a higher Mach number than 3.1 would eliminate this problem. Maximum payload is shown in figure 21 for a cowl capture area of 160 ft^2 during acceleration with the cruise capture area reduced to about 60 percent of this value or 96 ft^2. As with the first method of varying the cowl capture area, cowl drag and additional weight eliminate the advantages of resizing the capture area at cruise, but there is no significant loss in payload.

Figure 22 summarizes the results in terms of payload. The curve showing performance when cowl wave drag is ignored indicates the potential gain when resizing capture area at cruise. This gain is about 8 percent of the baseline payload. If cowl drag, cowl lift, and additional weights are considered, pivoting the cowl inward to reduce the capture area at cruise results in penalties that reduce the payload to less than that for the baseline. Pivoting the cowl outward to increase the capture area during acceleration results in penalties that reduce the payload to approximately the level of the baseline system for a capture area greater than 155 ft^2.

Reduced ramjet fuel-air ratio during cruise– For the propulsion system with a fixed cowl capture area throughout climb and cruise, it is possible to decrease the cruise altitude and thereby increase the vehicle lift-drag ratio at cruise by throttling to reduce the ramjet fuel-air ratio, as shown in figure 23. The resulting increase in payload is shown in figure 24. The increase in payload is more than 20 percent of the baseline payload and is due to improved propulsion system specific impulse as well as the increase in the vehicle lift-drag ratio. The specific impulse of the ramjet during cruise at Mach number 6 increases from 3550 sec to 3900 sec as the ramjet fuel-air ratio is decreased from stoichiometric to 0.02. This increase is due primarily to an increase in the propulsive efficiency of the ramjet.

It may not be possible to run the propulsion system at fuel-air ratios much less than stoichiometric due to engine and inlet cooling requirements. However, the parallel turbojet-ramjet propulsion system will minimize regenerative cooling requirements because the turbojet and a large portion of the inlet subsonic duct are closed off after the turbojets are shut down and need not be regeneratively cooled.

Inlet spillage during cruise– Another method of increasing the vehicle lift-drag ratio during cruise is to spill some of the inlet flow around the cowl. Spilling air around the inlet creates an additional lift force on the inlet ramps as well as drag, and thus the basic lift-drag relationship of the aircraft is altered slightly. The problem of cruising with an oversized capture area is that the aircraft must cruise at a higher altitude to balance thrust and drag, and this means that angle of attack must be increased to balance lift and weight. Thus, the spillage forces can be beneficial in two ways: the additional drag requires more thrust, resulting in a lower cruise altitude; and the additional lift will result in a lower angle of attack. The effect of increased inlet spillage on the vehicle lift-drag ratio is shown in figure 25, and it can be seen that the maximum cruise lift-drag ratio is approached as the inlet spillage flow ratio is increased to 0.3 (ratio of spilled flow to the total captured flow). The methods used to compute spillage forces are discussed in appendix A. The spillage forces themselves are accounted for as propulsion forces, and therefore the increase shown in figure 25 for the vehicle lift-drag ratio is simply the result of a decrease in cruise altitude. If the spillage forces were accounted for as aerodynamic forces, then the curves in figure 25 would intersect at an inlet spillage

flow ratio of approximately 0.2 which corresponds to the maximum payload as shown in figure 26. Payload increases by approximately 8 percent as the spillage flow ratio increases up to 0.2. A further increase in the spillage ratio results in a drop in payload due to degradation of the propulsive forces.

Ramjet Exhaust Flow Considerations

It has been assumed for the baseline system that the aft surface of the vehicle will be used for expansion of the ramjet exhaust gas in a one-dimensional, shifting equilibrium flow. The nominal all-body vehicle has an exit area to capture area ratio of approximately 4.5 based on a projection of the ramjet side plates and lower surface parallel to the vehicle centerline. Figure 27 shows the result of assuming different exit areas for the ramjet flow. Ideal expansion for a cruise Mach number of 6 is a ratio of nozzle exit area to cowl capture area of approximately 4, and therefore the baseline system inherently assumes ideal expansion of the ramjet exhaust after turbojet shutdown (a 2 percent loss for friction and divergence is included). A more complete discussion of the exhaust flow assumptions is given in appendix A. Payload drops off rapidly if the exit area to capture area ratio is less than 2. For example, if the area ratio is limited to 1.5 throughout acceleration and cruise, as it is while the turbojet is operating, then payload is reduced to 60 percent of the nominal value. Clearly, efficient expansion of the ramjet exhaust under the vehicle aft surface is a very critical factor which unfortunately is supported by little analytical or experimental work.

The reduction in payload if the exhaust flow gas constituents are assumed to be frozen at the ramjet nozzle throat throughout acceleration and cruise is shown in figure 28. The loss in payload is considerable, but it is doubtful that the flow would be completely frozen at a cruise Mach number of 6. The assumption of equilibrium flow is not validated by analytical and experimental work, and it is expected that the actual performance will lie somewhere between the two curves in figure 28. The interaction between the ramjet exhaust and the aft vehicle surface, along with the chemical kinetics in the nozzle, are extremely important, and gross assumptions concerning the nature of the exhaust flow are presently necessary because of the lack of experimental data.

Engine Installation Considerations

The baseline propulsion system has the maximum number of engines arranged side by side beneath the vehicle. To provide space for the landing gear, the total width of this engine package is limited to 87 percent of the vehicle width at the beginning of the inlet ramps. The ramjets are placed beneath the turbojets, and the width-to-height ratio of the ramjet duct is varied to balance the width of the ramjets and total propulsion system width.

A sketch of the baseline propulsion system, roughly to scale, is shown in figure 29, with pertinent dimensions defined. The inlet throat is arbitrarily placed at the vehicle breakpoint. The drawing shows the propulsion system package cutting into the original all-body vehicle with possible adverse effects on the design of the LH_2 tankage. If the tank problem is severe, the beginning of the inlet ramps could be placed at the vehicle breakpoint, and the propulsion package could fit under the vehicle without affecting the original all-body shape. For the baseline system this amounts to translating the propulsion package approximately 10 feet to the rear. Moving the engines to the rear would increase the boundary layer thickness at the inlet due to the longer length

from the vehicle bow, and it might lead to structural weight penalties due to a shift in weight away from the center of gravity of the vehicle. The required center of gravity of the all-body vehicle is slightly ahead of the breakpoint as shown in figure 1.

The effect of not using the maximum allowable span for engine installation is shown in figure 30. As the number of engines is decreased, less span is used for inlet width as shown in figure 30(a), and for a constant capture area the cowl height increases proportionally. The effect of the number of engines on the inlet and engine weight fractions is shown in figure 30(b). As the number of engines decreases from a maximum of 14, the inlet weight remains about the same, but engine weight increases. Thus, the reduced payload with a decreasing number of engines shown in figure 31 is due to an increase in total engine weight. Included in the analysis of engine number effect on payload is the fact that the boundary layer thickness becomes less of a factor in engine performance with a decreasing number of engines due to increased cowl height and decreased inlet width. Nevertheless, there is a 10 percent decrease in payload as the number of engines is decreased from 14 to 4. If it were necessary to divert the boundary layer rather than ingest it into the inlet, it might be desirable to reduce the number of engines, thereby minimizing the width of the inlet.

The baseline system is characterized by minimum height H_{prop}, and length, X_{prop}, as well as maximum width W (defined in fig. 29). The effect of engine number on the length and height is shown in figure 32. The total length is broken down into inlet, diffuser, and engine lengths in figure 33. Figure 34 shows scaled drawings of the propulsion system installed in the all-body vehicle for 14 (baseline), 10, and 6 engines. It is evident that the number of engines should be maximized to keep installation length and height at a minimum.

Evaluation of the Wraparound Turboramjet

Wraparound turboramjets have been used extensively in previous hypersonic airplane studies. They are particularly attractive for use with an axisymmetric inlet because of their circular cross section, but they are not well suited for use with a two-dimensional inlet because the large diameter of the engine leads to an excessively long and heavy subsonic diffuser. This fact is demonstrated in the evaluation that follows. This evaluation compares the wraparound turboramjet with the baseline turbojet-ramjet system, both having two-dimensional inlets installed on an all-body vehicle.

The wraparound turboramjet has an annular ramjet wrapped around the gas generator with concentric exhaust nozzles. Because of the annular ramjet nozzle, it would be difficult to design a lightweight system that would enable the ramjet exhaust to expand under the all-body vehicle in an efficient manner. Thus, for this study, wraparound turboramjet thrust is computed for expansion of the ramjet exhaust to an exit area equal to the maximum engine cross-section area. This assumption combined with the heavier weights associated with the wraparound turboramjets degrades payload severely, as shown in figure 35(a).

The results of figure 35(a) are pessimistic because there will be some added thrust due to expansion beneath the vehicle; but it is fair to compare these results with those of the baseline turbojet-ramjet system having the ramjet exhaust gas expanding only beneath the turbojets (i.e., out to point A in fig. 2). Limiting the expansion to this point results in a ratio of nozzle exit area to cowl capture area of 1.5. Baseline payload for this area ratio is also shown on figure 35(a) and is much greater than the maximum payload of the wraparound turboramjet. The exit area of the

wraparound turboramjet is usually defined by the ratio of the maximum ramjet nozzle throat area to the sea level static maximum airflow. The curves in figure 35(b) relate this ratio to the ratio of cowl capture area to maximum ramjet nozzle throat area for direct comparison with the baseline turbojet-ramjet system. It can be seen that in all cases, the area ratios for the wraparound turboramjet corresponding to the payload data shown in figure 35(a) are greater than 1.5.

Weights and dimensions of the wraparound turboramjets are shown in figures 36 and 37, respectively. Note that these weights and dimensions are for installations with the maximum number of engines. The annular configuration of the ramjet increases the engine diameter, which decreases the number of engines that can fit beneath the vehicle and increases all propulsion system dimensions and weights over those for the baseline turbojet-ramjet system (indicated by the circular symbols).

CONCLUSIONS

This study has presented an evaluation of a turbojet-ramjet propulsion system installed on an all-body vehicle that cruises at a Mach number of 6.0. The configuration of the vehicle has been kept fixed throughout the study, and a baseline propulsion system has been defined. Various characteristics of the propulsion system have been changed from the baseline definition in an attempt to identify the effect of the propulsion system design on the aircraft payload.

Conclusions 1 through 5 are concerned with the sizing of the cowl-capture area and the turbojet and ramjet engines.

1. The high transonic drag characteristic of the baseline all-body vehicle dictates the size of the turbojets and the cowl capture area and results in take-off thrust to vehicle gross weight ratios greater than 1.1.

2. Payload is relatively insensitive to capture area size as long as the turbojet engine demand for air does not exceed the inlet supply transonically. However, the payload is increased if the inlet is sized to provide some transonic ramjet thrust.

3. The ramjet is sized by acceleration requirements during the climb trajectory rather than at the cruise point. The minimum ramjet size is dictated by the thrust required to accelerate after the turbojets are shut down. In this study, the turbojet shutdown Mach number was varied between 3.0 and 4.0.

4. There is an optimum combination of ramjet size and turbojet shutdown Mach number that maximizes payload.

5. Increasing inlet pressure recovery transonically has a large effect on payload because the turbojets are sized at this point.

For the baseline propulsion system, the ramjet fuel-air ratio is defined as stoichiometric throughout acceleration and cruise, and the cowl capture area is not variable. Since the capture area is sized transonically, the aircraft does not cruise at the altitude for maximum vehicle lift-drag ratio

with the baseline propulsion system. Conclusions 6 through 8 are concerned with methods of improving payload by bringing the aircraft lift-drag ratio closer to the maximum.

6. A modest gain in payload is potentially available if a variable capture area inlet is employed and resized at cruise to fly at maximum vehicle lift-drag ratio. However, this potential gain was lost for the baseline vehicle design used in this study due to cowl drag and weight penalties.

7. For a constant capture area throughout the flight, significant payload increases can be obtained by running the ramjets at a lean fuel-air ratio during cruise, if propulsion system regenerative cooling requirements permit.

8. For a constant capture area throughout the flight, spillage of some of the inlet flow around the cowl during cruise can increase payload.

The remaining conclusions drawn from the results of this study are as follows:

9. Payload can be greatly influenced by the nature of the exhaust flow expanding under the vehicle afterbody; specifically, the assumption of ideal expansion of the exhaust flow beneath the vehicle afterbody and the assumption of shifting equilibrium flow in the exhaust have not been substantiated by analytical and experimental work.

10. Arranging the maximum number of engines to span the vehicle width has the effect of minimizing the propulsion system weight, height, and length, thus increasing the payload.

11. The wraparound turboramjet with a two-dimensional inlet is not a suitable engine for the all-body vehicle.

National Aeronautics and Space Administration
Moffett Field, Calif. 94035, July 9, 1970

APPENDIX A

PROPULSIVE FORCES

Lift and drag forces are computed for an aerodynamically clean all-body vehicle as shown in figure 38. The methods used to compute these forces are described in reference 8. In the present analysis of the propulsion system, the vehicle in supersonic flight is treated as a two-dimensional wedge. The static pressure under the vehicle forebody p_1 and the inviscid total pressure ahead of the inlet p_{T_1} are obtained through oblique shock relations. In subsonic flight, these pressures are assumed equal to free-stream static and total pressure, respectively.

Figure 39 shows the propulsion system free body used for a parallel turbojet-ramjet arrangement of the engines. No expansion beneath the vehicle is assumed for the turbojet exhaust because the turbojet nozzles are circular. Thus, with the turbojet operating, the free body is drawn vertically through the exit of the turbojet and ramjet nozzles, and the ramjet exhaust expands only beneath the turbojet. When the turbojets are off, the two-dimensional flow from the ramjets is assumed to expand beneath the entire vehicle afterbody, and the free body is drawn through the trailing edge of the vehicle normal to the center line. The maximum exit area is bounded on the bottom by the plane projected from the ramjet parallel to the vehicle center line, on the top by a horizontal plane through the center line, and on the sides by vertical planes through the side plates of the propulsion system. If the ideal exit area is less than this maximum, the free body is drawn to the ideal exit area as shown in figure 39; that is, the exhaust flow is never overexpanded. The free body for the wraparound turboramjet is identical to figure 39 except no expansion beneath the vehicle is assumed for the ramjet exhaust gas throughout the flight, since the exhaust nozzle is annular.

To completely account for the forces around the propulsion free body shown in figure 39, an additional force should be included in the net thrust equation which would account for the difference in the base pressure p_b, and free stream static pressure p_0. This force would be:

$$\text{Base drag correction force} = p_0[(p_b/p_0) - 1](A_{\text{aft surface}})\sin(\Delta_b - \alpha) \qquad \text{A1}$$

This force has been ignored in computing net thrust, and the error introduced is small so long as the compression of air through the forebody shock field is approximately cancelled by the isentropic expansion around the corner of the vehicle breakpoint; or when the aft surface is approximately parallel to the direction of flight (i.e., angle of attack α is equal to the after surface angle Δ_b, see fig. 38). During climb and acceleration along the baseline trajectory, the base pressure computed from clean-body aerodynamics is always less than free stream static pressure, and the base drag correction force would increase net thrust by 3 to 9 percent depending upon the point on the trajectory. During cruise, angle of attack is greater than the aft surface angle, and in this case the base pressure computed from clean-body aerodynamics is higher than free-stream static pressure because of the high compression of the forebody shock. However, the aft surface is facing forward because the angle of attack is larger than the aft surface angle. Thus the base drag correction force would again increase net thrust – in this case by about 4 percent. An accurate computation of the vehicle base pressure forces resulting from expansion of the engine exhaust gas would require a detailed method of characteristics solution.

The additive drag force due to spillage of inlet flow around the cowl lip is accounted for with the empirical drag coefficient plotted in figure 40 which is representative of current variable geometry supersonic inlets. Lift due to spillage is obtained by treating the outer streamline after the first inlet shock as a ramp surface and computing the lift component of the force (see the sketch in fig. 41). The original lift force must be subtracted from this spillage lift and is computed from the all-body aerodynamics over an area equal to a projection of the spillage area normal to the lift direction. This analysis assumes that the normal shock in the mixed flow inlet is maintained inside the inlet downstream of the throat as shown in figure 41. If the normal shock is forced out ahead of the cowl, then the external inlet flow no longer forms a single ramp surface and computations as outlined above are invalid.

To compute the supersonic cowl forces, the cowl is treated as a flat plate at an angle of attack to the body shock wave flow field, as shown in figure 42. When the cowl is pivoted inward, the angle of attack is positive and cowl pressure coefficient is computed from oblique shock relationships. When the cowl is pivoted outward, the angle of attack becomes negative, and the pressure coefficient in a supersonic flow field is computed assuming a Prandtl-Meyer expansion around the cowl lip. In a subsonic flow field, the empirical pressure coefficient shown in figure 43 is used. This pressure coefficient was obtained by fairing a curve between the data from reference 9 for incompressible air (Mach number less than 0.6) and the pressure coefficient computed for an isentropic expansion at Mach number 1. To compute the cowl pressure coefficient at a subsonic local Mach number, M_1, the pressure coefficient is determined for a Prandtl-Meyer expansion around the cowl for a local Mach number of 1.0. This would be $C_{p_{1.0}}$. The curve in figure 43 is then used to compute $C_{p_{M_l}}$. For supersonic Mach numbers the actual flow field is complicated by the fact that the inlet shock does not intersect the cowl lip for local Mach numbers less than 3.0. The external flow is compressed, turned parallel to the first inlet ramp by the initial ramp shock, and then expanded around the cowl lip. However, to simplify the computation during the trajectory calculations, the shock is assumed to be on the cowl lip at all supersonic Mach numbers, and the expansion is assumed to be from the forebody flow field. A separate analysis demonstrated that this assumption leads to a 1 to 2 percent error in the pressure coefficient.

Gross thrust was calculated in separate computer programs for the turbojet, ramjet, and the turboramjet. The turbojet and turboramjet programs were generated from the data given in references 5 and 6, respectively. These data give curves of specific gross thrust, defined as the ratio of gross thrust to compressor airflow, and a gross thrust coefficient, which accounts for friction and divergence in the nozzle as well as underexpansion losses for a given nozzle area ratio. The ramjet computer program calculates gross thrust and thrust coefficient based on the ramjet thermodynamic cycle for given inputs of maximum nozzle throat area, nozzle exit area, duct area, and fuel-air ratio. This program was used to generate a second program for the all-body vehicle synthesis, which used curves of specific gross thrust and gross thrust coefficient in the same format as in the turbojet and turboramjet programs.

The equations used to compute the net propulsive forces along the vehicle center line (thrust) and normal to the vehicle center line (lift) are as follows:

(1) Gross thrust, F_G, is given by

$$(F_G/Wa)_{ideal} = f_1\left(T_{T_2},\ p_{T_N}/p_0,\ f/a\right) \tag{A2}$$

$$C_T = f_2\left(p_{T_N}/p_0,\ A_{ex}/A_T\right) \tag{A3}$$

$$F_G = (F_G/Wa)_{ideal}(Wa)(C_T) \tag{A4}$$

Gross thrust for both engine types is directed parallel to the body centerline.

(2) The ram drag, D_R, is given by

$$D_R = \frac{WaV_1(1 - \theta/H_{cwl})}{g} + (p_1 - p_0)A_1 \tag{A5}$$

and is directed parallel to the lower forebody surface.

(3) The net propulsive force, F_D, is given by

$$F_D = F_G \cos\alpha - (D_R + D_{spill} + D_{cwl})\cos(\alpha + \Delta_1) - (L_{spill} + L_{cwl})\sin(\alpha + \Delta_1) \tag{A6}$$

(4) The net propulsive lift force, F_L, is given by

$$F_L = F_G \sin\alpha - (D_R + D_{spill} + D_{cwl})\sin(\alpha + \Delta_1) + (L_{spill} + L_{cwl})\cos(\alpha + \Delta_1) \tag{A7}$$

APPENDIX B

PROPULSION SYSTEM WEIGHTS

By definition, the propulsion system includes the engines, inlets, firewalls between engines, engine nacelles, sidewalls in the ramjet exhaust region, and the ramjet exhaust expansion surface beneath the turbojets. Turbojet weight and turboramjet weight are estimated from empirical scaling data given in references 5 and 6, respectively. Ramjet weight is computed from the following equation

$$W_{RJ} = 111(A_{D_{RJ}}) \tag{B1}$$

The unit weight of 111 lb/ft^2 of ramjet duct area is a figure suggested in reference 2 for ramjets with circular cross section. There are no weight data for the type of ramjet proposed in this study, that is, a strictly two-dimensional duct and nozzle. Figure 44 relates the unit weight based on the duct cross-sectional area to a unit weight based on the internal surface area of the ramjet duct for given values of a length factor defined as the ratio of the ramjet length to an equivalent diameter

$$K_L = \frac{L_{RJ}}{\sqrt{4A_{D_{RJ}}/\pi}} \tag{B2}$$

For example, at a length factor of 2.0 and a duct width-to-height ratio of 2.0, a unit weight of 111 lb/ft^2 of duct cross-sectional area corresponds to approximately 11.5 lb/ft^2 of duct surface area. Presumably a two-dimensional ramjet would be constructed in much the same manner as is the subsonic diffuser of a two-dimensional hypersonic inlet, that is, a load-carrying structure with a bonded or mechanically attached heat exchanger through which the LH_2 fuel flows. This type of construction is discussed in reference 10 which suggests a weight per unit surface area of 7.7 lb/ft^2 for a panel with a mechanically attached heat exchanger under a load of 250 psi and a heat flux of 500 Btu/ft^2 sec. The duct pressure for this study was limited to 200 psi, but in the present case, the heat flux in the ramjet would be higher because of the increase in gas temperature and convective heat transfer coefficient in the ramjet duct. With the additional weight of the heat exchanger manifolds, the fuel lines and nozzles into the duct, and the structure in the nozzle throat region, 11 to 12 lb per unit duct surface area appears to be a realistic unit weight. The effect of ramjet unit weight on the payload of the baseline system of this study is shown in figure 45 for a range of unit weights from 70 to 150 lb per unit duct cross-sectional area. The range in payload variation is 6 percent of the nominal payload, which is significant in relation to the other propulsion parameters evaluated in this study.

The remainder of the propulsion system weights are lumped into inlet weight, which would include the weights of external and internal inlet ramps; sidewalls and splitters (which split the flow from the beginning of the first inlet ramp completely through the propulsion system and out along the expansion surface of the ramjets beneath the turbojets); cowl; subsonic diffuser; door to seal off the turbojet duct; transition ducting to the turbojets; external panel beneath the propulsion system, which could be considered a nacelle; expansion surface beneath the turbojets for the ramjet exhaust flow; thermal protection panels for all internal ducting exposed to the flow at a free-stream Mach number greater than 4.5; inlet cooling manifold systems; and inlet actuators and controls.

The evaluation of weights for a two-dimensional inlet was based on the inlet design and unit weights published in reference 7. Scaled drawings of the inlet at flight Mach numbers of 6, 3, and 1.1 are shown in figure 46. Actuators are shown schematically in the Mach 6 and Mach 1.1 sketches and do not represent an actual design.

The results of the weights evaluation are shown in figure 47 for a cruise Mach number of 6 for both the parallel turbojet-ramjet and wraparound turboramjet engine systems. Inlet unit weights for the turboramjets increase by 160 lb/ft^2 as the ratio of maximum nozzle throat area to capture area is increased from 0.3 to 0.9. This is due to the increase in engine diameter, which results in a longer subsonic diffuser from the inlet throat to the engine face. Inlet unit weights for the separate turbojet-ramjet system also increase with ramjet size but are not as sensitive. Increasing the ratio of maximum nozzle throat area to capture area from 0.3 to 0.9 increased the inlet unit weight by only 45 lb/ft^2.

Side plates separate the inlets of each individual engine from the beginning of the external ramps to the engine faces. For both engine systems it is assumed that the diffuser sidewalls exposed to the flow for a flight Mach number of 4.5 or greater must be regeneratively cooled. Since the turbojet ducting is valved off at a flight Mach number less than 4 for the separate turbojet-ramjet system, the area of cooled panels required is much less than that for the wraparound turboramjets, which leads to a considerable saving in weight. For example, the thermal protection system in the inlet of the baseline turbojet ramjet system weighed 4325 lb. The thermal protection system in the inlet of a wraparound turboramjet for the same capture area, a maximum number of engines, and the smallest ramjet annulus (ratio of maximum nozzle throat area to sea-level static airflow of 0.014) weighed 8710 lb.

To assess the effect of the thermal protection system weight on the unit weight of the inlet, one can consider lower Mach number cruise conditions. For a cruise Mach number of 5, no cooled panels are needed on the inlet external ramps, and for a cruise Mach number of 4, no regenerative cooling is required throughout the inlet. Inlet unit weights modified for these lower cruise Mach numbers are also shown in figure 47.

Figure 48 uses the data from figure 47 to demonstrate that weight for these two-dimensional inlets is primarily a function of the turboaccelerator sea-level-static airflow which is a convenient measure of engine size. In reality, the turbine engine diameter, not the capture area, is the dominating factor in the weight of the inlet because both the subsonic diffuser, which is the heaviest section in the inlet due to its length, and the sidewalls between engines, increase in length, and therefore weight, directly with the engine diameter.

Additional actuator and control weight is added to inlet weight for the variable capture area inlet designs shown in figure 42. This additional weight is assumed to be linear with the length of the movable cowl according to the following equation:

$$\Delta W_{INL} = 22A_c(L_{cwl}/H_{cwl})/6 \tag{B3}$$

where

$$H_{cwl}/L_{cwl} = \sin \delta \tag{B4}$$

APPENDIX C

BOUNDARY–LAYER CALCULATIONS

The momentum thickness of the boundary layer is computed so that the ram drag due to the momentum of the inlet airflow can be corrected as shown in appendix A. The displacement thickness is calculated to correct the quantity of airflow into the inlet and the total pressure at the beginning of the inlet. The following equations for a turbulent boundary layer, with the exception of compressibility effects, can be found in reference 11.

Momentum thickness θ is given by

$$\theta = \frac{C_{F_I} \ell (C_F/C_{F_I})}{2} \tag{C1}$$

where

$$C_{F_I} = [0.455/(\log_{10} R_\ell)^{2.58}] - 1700\, R_\ell' \tag{C2}$$

and

$$R_\ell = \rho_e u_e \ell / \mu_e \tag{C3}$$

Compressibility effects are evaluated using the "T prime" method (ref. 12) with Eckert's coefficients (ref. 12)

$$T'/T_e = 0.5 + 0.5(T_w/T_e) + 0.0396\, M_\ell \tag{C4}$$

$$F_c = C_{F_I}/C_F = T'/T_e \tag{C5}$$

$$F_R = R_\ell'/R_\ell = (\rho' \mu_e)/(\rho_e \mu) = (T_e/T')(\mu_e/\mu') \tag{C6}$$

where the viscosity ratio is given by Sutherland's equation

$$(\mu'/\mu_e) = (T'/T_e)^{1.5}(1 + 198.6/T_e)/[(T'/T_e) + 198.6/T_e] \tag{C7}$$

The wall temperature T_w, in equation (C4) is computed as the mean radiation equilibrium temperature on the lower forebody surface of the all-body vehicle.

The displacement thickness is given by the equation

$$\delta^* = \delta/(1 + n) \tag{C8}$$

where n is the exponent used to correlate the velocity profile of the turbulent boundary layer to the distance from the wall.

$$(u/u_e) = (y/\delta)^{1/n} \qquad (n = 7 \text{ is typical}) \tag{C9}$$

The boundary-layer thickness δ is given by

$$\delta = C_F(\ell/2)(\theta/\delta) \tag{C10}$$

where C_F is given above and (θ/δ) is given by

$$(\theta/\delta) = n/[(1 + n)(2 + n)] \tag{C11}$$

To compute the inlet airflow and total pressure at the beginning of the inlet the following procedure is used:

1. Compute the local Mach number in the shock field for local inviscid conditions

$$z = M^2\left(1 + \left\{[(\gamma - 1)/2]M^2\right\}\right) = \left[(Wa/A_c)_{INV}\right]^2 (RT_T/\gamma g p_s{}^2) \qquad (C12)$$

For $\gamma = 1.4$

$$M^2 = -2.5 + (1 + 0.8z)/0.4 \qquad (C13)$$

2. Compute the local total pressure in the shock field for the local inviscid flow conditions

$$p_{T_{INV}} = p_s \left(1 + \frac{\gamma - 1}{2} M^2\right)^{\frac{\gamma}{\gamma - 1}} \qquad (C14)$$

3. Compute a new value of weight flow per unit area at the beginning of the inlet ramps by including the displacement thickness of the boundary layer

$$(Wa/A_c)_{BL} = (Wa/A_c)_{INV}(h_{cw1} - \delta^*)/h_{cw1} \qquad (C15)$$

since capture area A_c, is a constant

$$(Wa)_{BL} = (Wa)_{INV}(h_{cw1} - \delta^*)/h_{cw1} \qquad (C16)$$

4. Compute $p_{T_{BL}}$ using equations (C12) and (C13) with $(Wa/A_c)_{BL}$ substituted for $(Wa/A_c)_{INV}$.

5. Compute the ratio of total pressure with boundary layer to the inviscid total pressure

$$R_{p_T} = \left(p_{T_{BL}}/p_{T_{INV}}\right) \qquad (C17)$$

During the trajectory computations a value of total pressure ahead of the inlet is computed for inviscid flow conditions along with R_{p_T}; then the inlet total pressure with boundary layer effects will be

$$\left(p_{T_{INL}}\right)_{BL} = \left(p_{T_{INL}}\right)_{INV}\left(R_{p_T}\right) \qquad (C18)$$

Figure 49 is a plot of the boundary layer correction factor for the total pressure ahead of the inlet R_{p_T} along the trajectory shown in figure 4.

REFERENCES

1. Gregory, T. J.; Petersen, R. H.; and Wyss, J. A.: Performance Tradeoffs and Research Problems for Hypersonic Transports. J. Aircraft, vol. 2, no. 4, July-August, 1965, pp. 266-271.

2. Jarlett, F. E.: Performance Potential of Hydrogen-Fueled Airbreathing Cruise Aircraft. 5 Volumes, Rep. GDC DCB 66-004/1 – 66-004/4 (General Dynamics/Convair – Contract NAS 2-3180), May-Sept. 1966.

3. Gregory, T. J.; Wilcox, D. E.; and Williams, L. J.: The Effects of Propulsion System – Airframe Interactions on the Performance of Hypersonic Aircraft. AIAA Paper 67-493, 1967.

4. Morris, R. E.; and Williams, N. B.: Study of Advanced Airbreathing Launch Vehicles With Cruise Capability, Volumes I – VI, Lockheed-California Company – Contract NAS 2-4084, Reps. NASA CR-73194 – 73199. Feb.-Apr. 1968.

5. Apel, G. F.; and Hines, R. W.: Estimated Performance of a Mach 4.0 Hydrogen Fueled Stoichiometric Turbojet (SRT233). TDM 2000, Pratt and Whitney Aircraft, Jan. 1967.

6. Apel, G. F.; and Hines, R. W.: Estimated Performance of a Mach 8.0 Hydrogen Fueled Wrap-Around Turboramjet (SWAT 201B). TDM 2001, Pratt and Whitney Aircraft, Jan. 1967.

7. Brewer, G. D.: An Analytical Investigation for the Application of Structural Concepts to Hypersonic Inlet Configurations. AFFDL–TR–68-87,vols. 1 and 2, Lockheed-California Co., July 1968.

8. Williams, Louis J.: Estimated Aerodynamics of All-Body Hypersonic Aircraft Configurations. NASA TM X–2091, 1970.

9. Eiffel, G. (J. C. Hunsaker, trans.): The Resistance of the Air and Aviation. Houghton-Mifflin, 1913.

10. Heldenfels, Richard R.: Structural Prospects for Hypersonic Air Vehicles. ICAS Paper 66-31, Sept. 1966.

11. Schlichting, Hermann (J. Kartin, trans.): Boundary Layer Theory, Fourth ed., McGraw-Hill Book Co. Inc., 1960.

12. Eckert, Ernst. R. G.: Survey on Heat Transfer at High Speeds. ARL Rep 189, Dec. 1961.

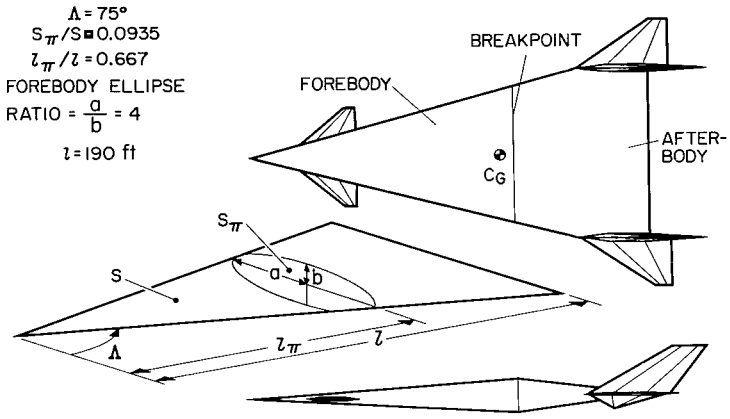

Figure 1.– All-body vehicle.

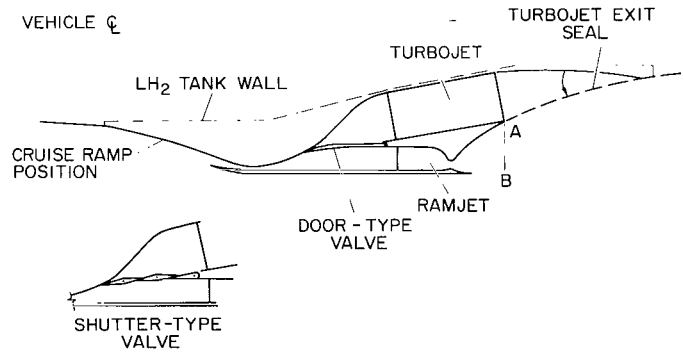

Figure 2.– Propulsion system.

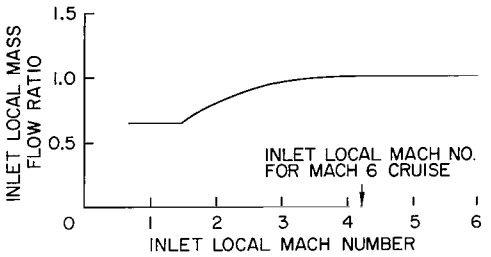

Figure 3.– Inlet mass-flow schedule.

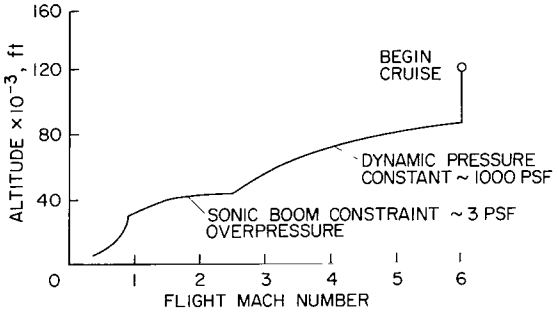

Figure 4.– Flight trajectory.

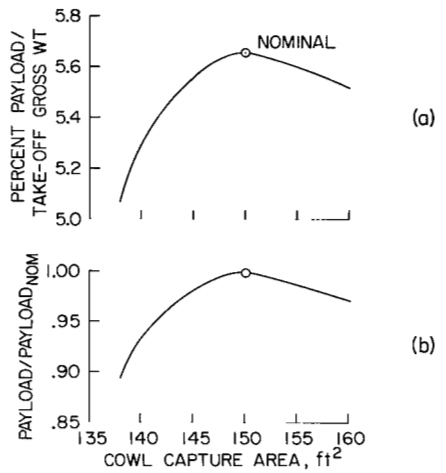

Figure 5.– Payload for baseline propulsion system.

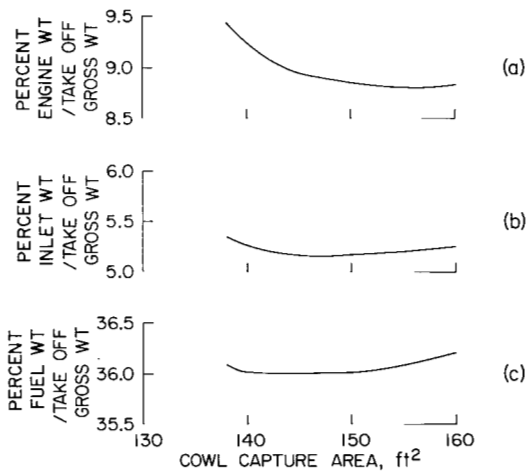

Figure 6.– Weight breakdown for fuel and propulsion system.

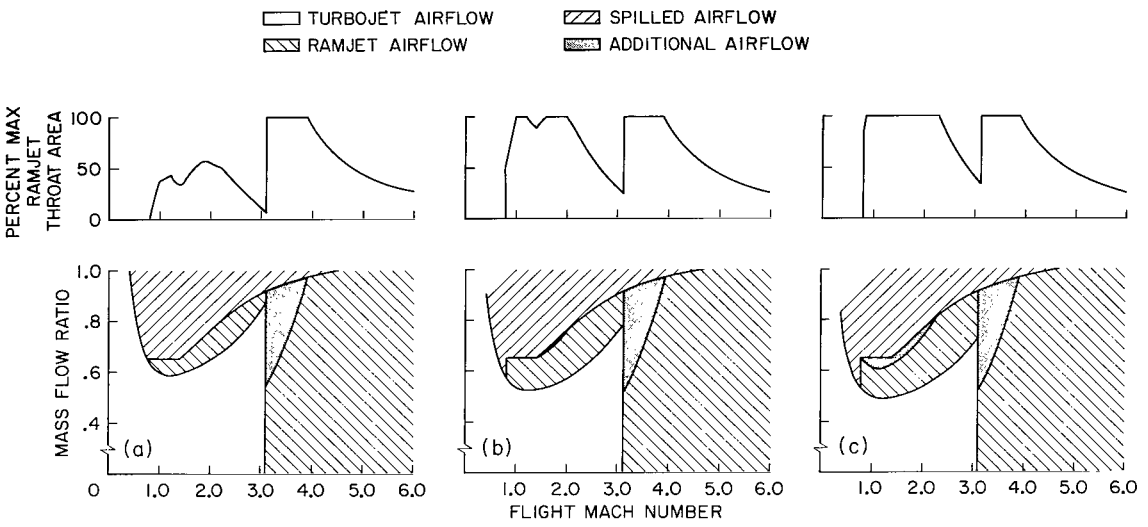

Figure 7.– Engine mass-flow ratio and ramjet throat (2 parts).

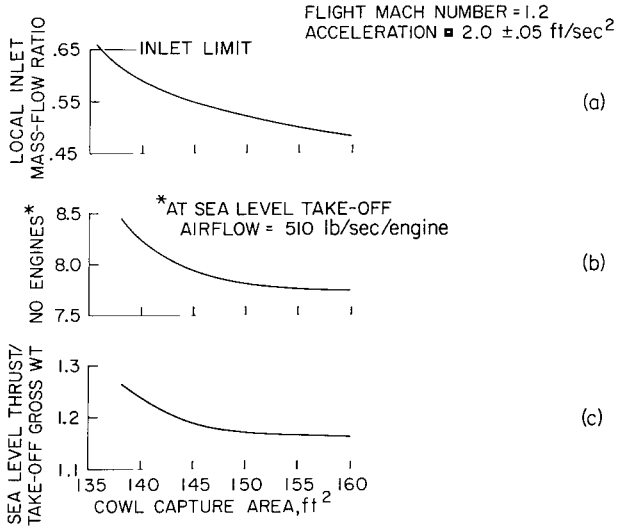

Figure 8.– Turbojet sizing at transonic pinch point.

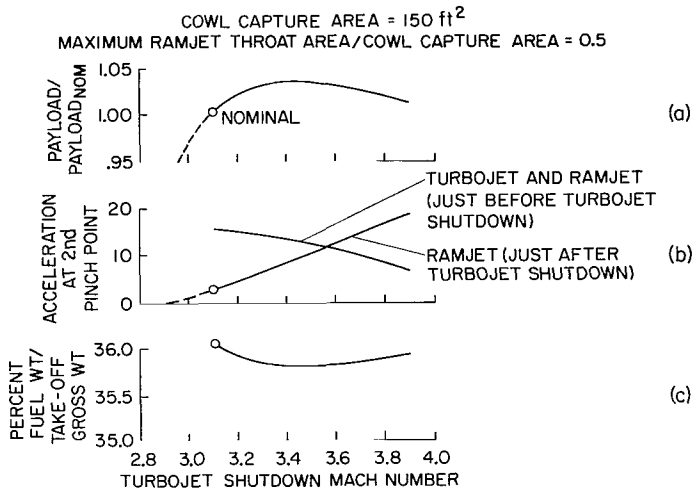

Figure 9.– Effect of turbojet shutdown Mach number.

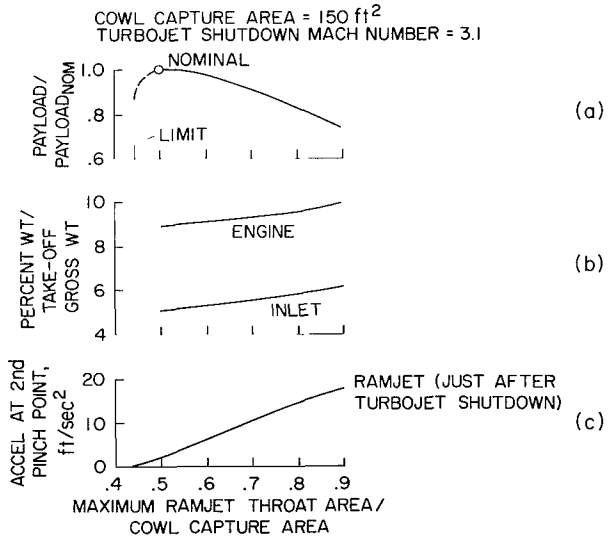

Figure 10.– Effect of ramjet size.

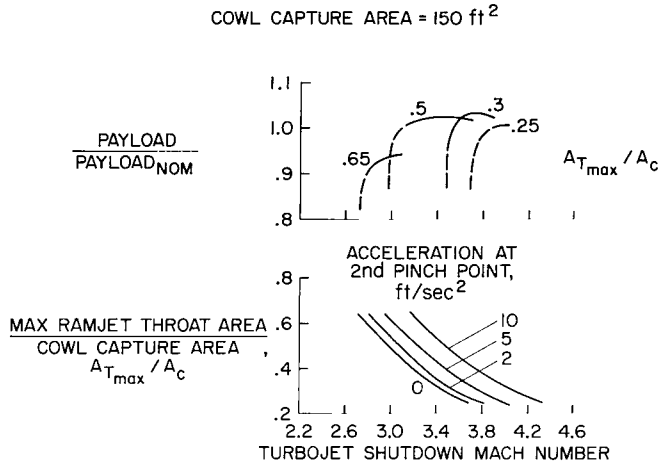

Figure 11.– Combined effect of ramjet size and turbojet shutdown Mach number.

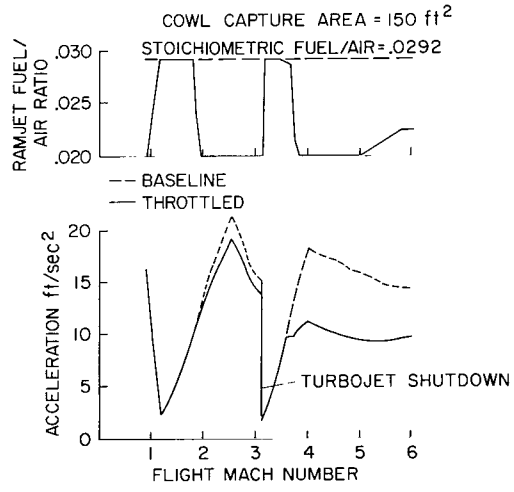

Figure 12.– Effect of throttling the ramjet on vehicle acceleration.

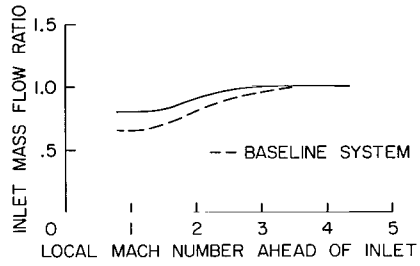

Figure 13.– Inlet schedule with increased transonic mass-flow ratio.

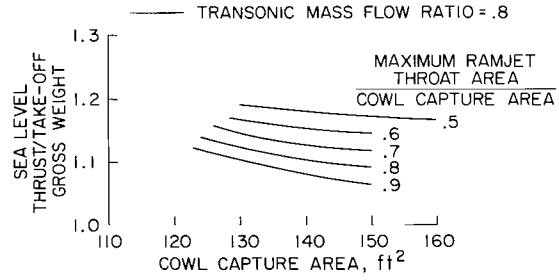

Figure 14.– Effect of increased transonic inlet mass-flow ratio on the ratio of sea-level thrust to take-off gross weight.

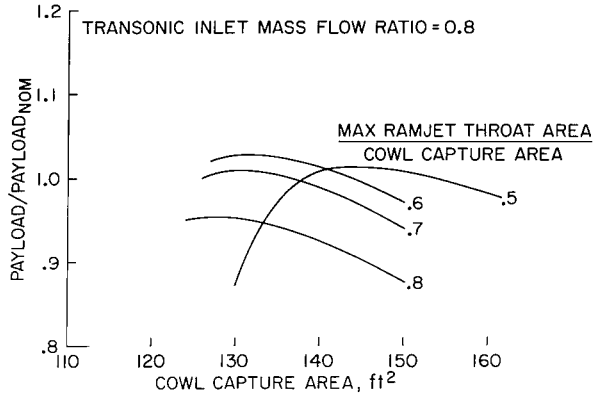

Figure 15.– Effect of increased transonic inlet mass-flow ratio on payload.

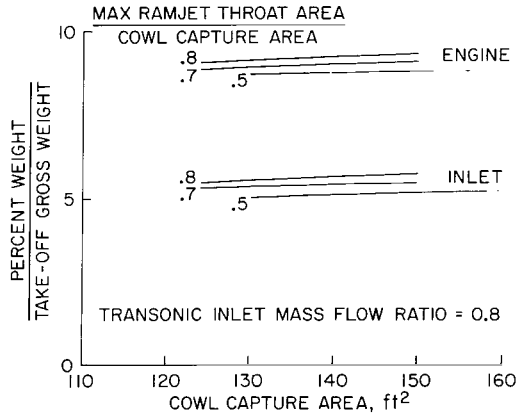

Figure 16.– Propulsion system weights for increased transonic inlet mass-flow ratio.

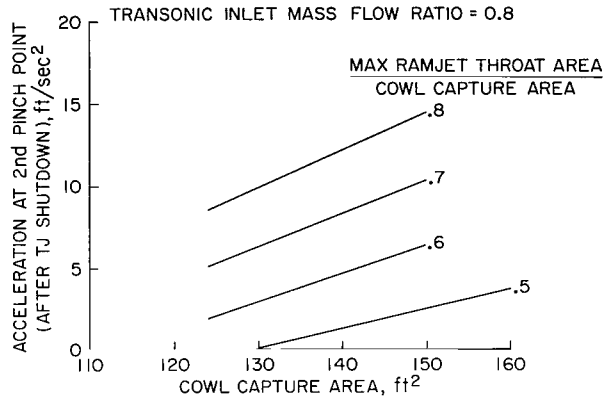

Figure 17.– Acceleration for increased transonic inlet mass-flow ratio.

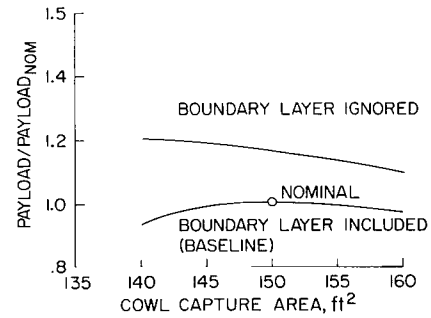

Figure 18.– Effect of inlet boundary layer on payload.

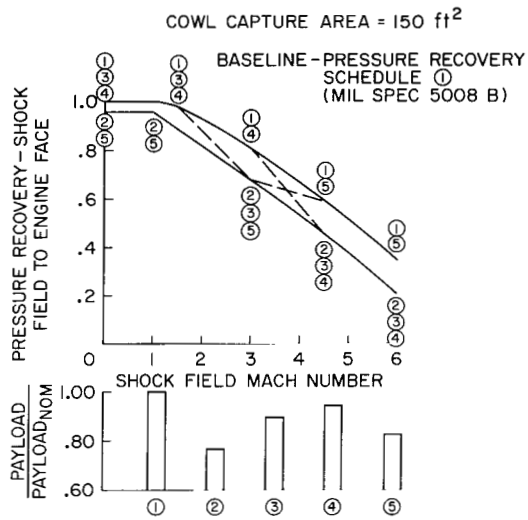

Figure 19.– Effect of inlet pressure recovery on payload.

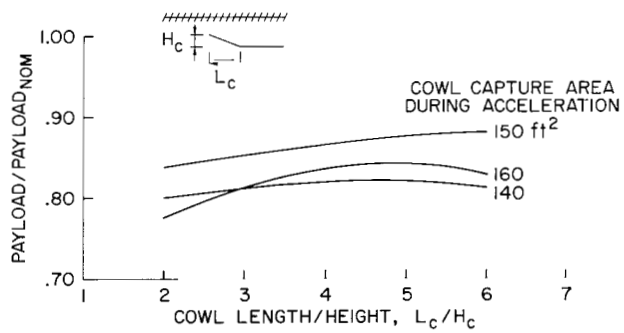

Figure 20.– Effect of resizing cowl capture area for cruise.

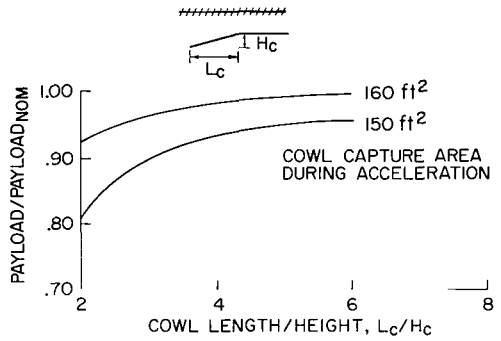

Figure 21.– Effect of resizing cowl capture area for acceleration.

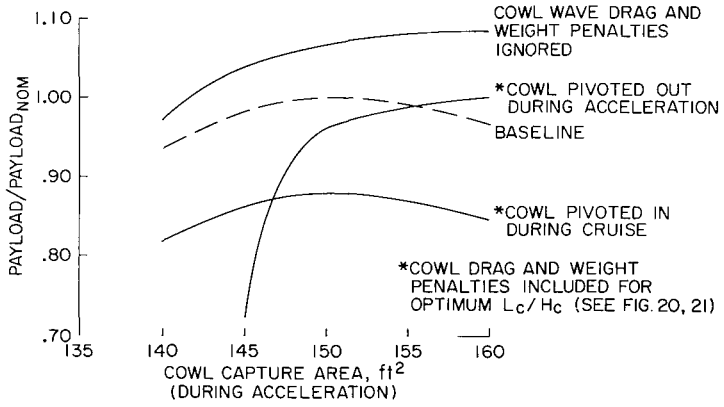

Figure 22.– Effect of resizing cowl capture area on payload.

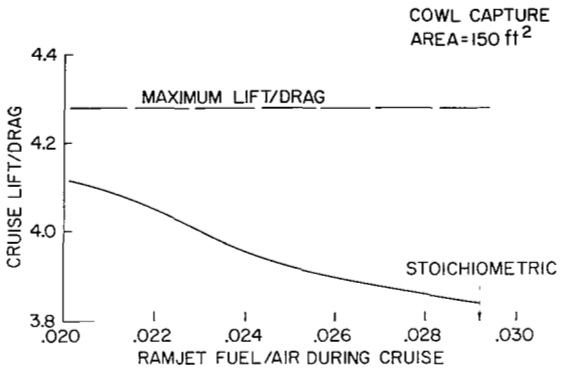

Figure 23.– Increase in vehicle lift-drag ratio with reduced cruise fuel-air ratio.

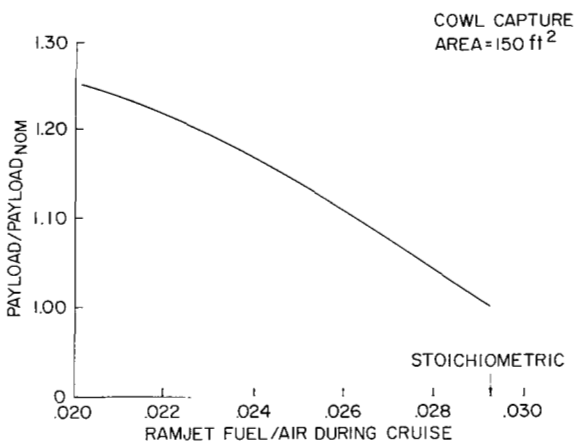

Figure 24.– Increase in payload with reduced cruise fuel-air ratios.

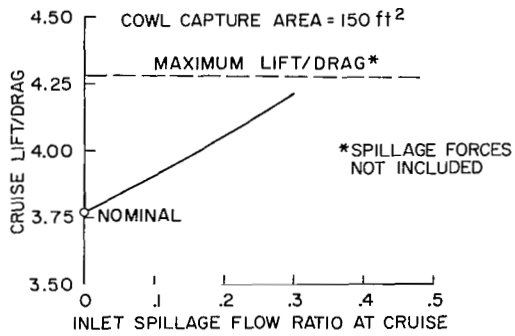

Figure 25.– Increase in vehicle lift-drag ratio at cruise with increasing inlet spillage.

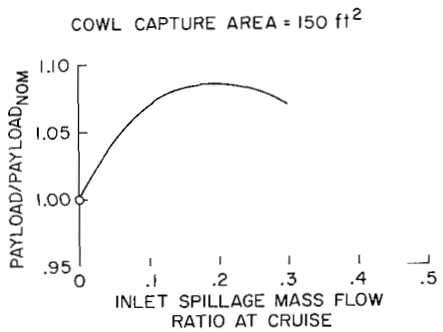

Figure 26.– Effect of inlet spillage on payload.

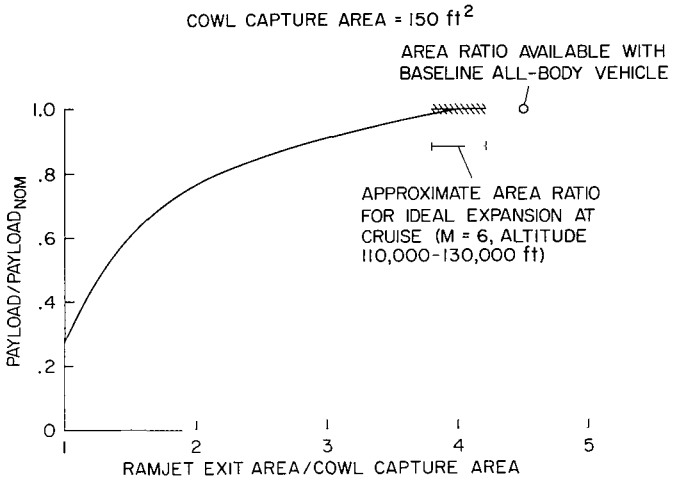

Figure 27.– Increase in payload with increase in nozzle exit area.

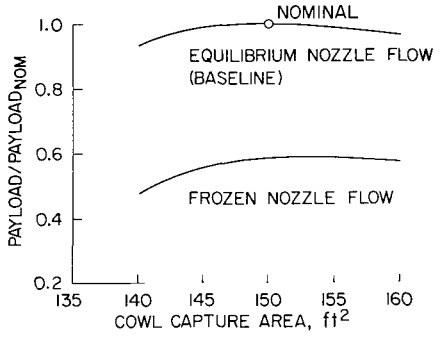

Figure 28.– Reduction of payload with ramjet nozzle frozen flow.

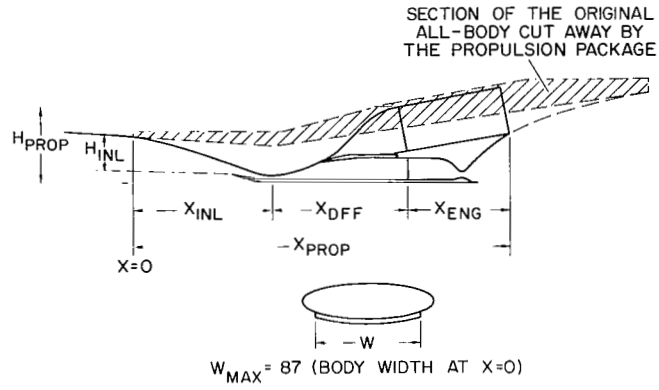

Figure 29.– Definition of baseline propulsion system installation dimensions.

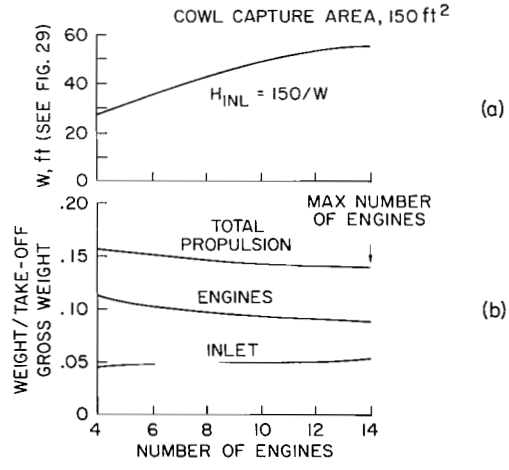

Figure 30.– Effect of number of engines on propulsion system with width and weight.

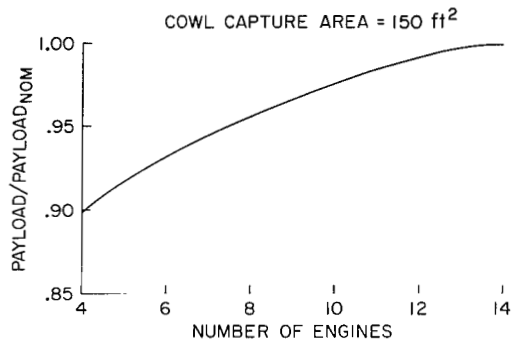

Figure 31.– Increase in payload with increasing number of engines.

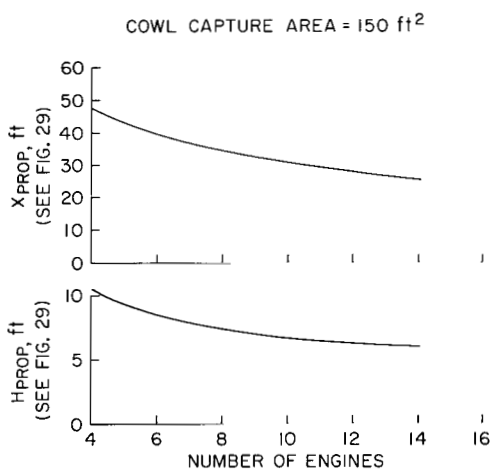

Figure 32.– Reduction in propulsion system height and length with increasing number of engines.

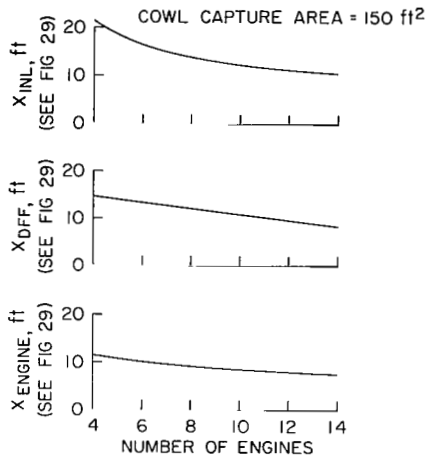

Figure 33.– Breakdown of propulsion system length.

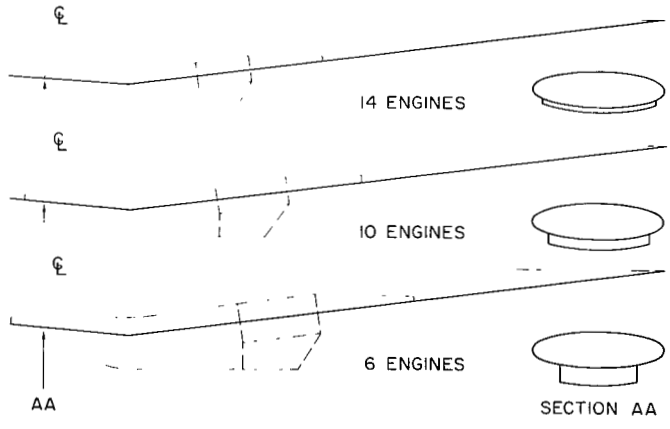

Figure 34.– Effect of number of engines on installation requirements.

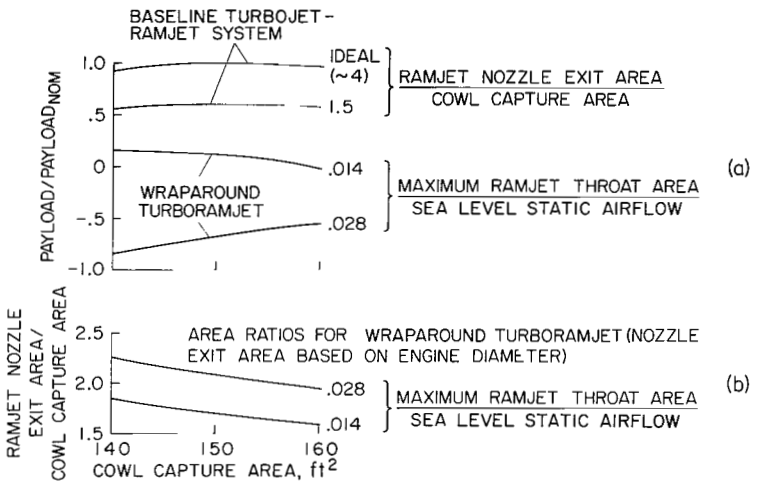

Figure 35.– Payload comparison between baseline turbojet-ramjet system and the wraparound turboramjet.

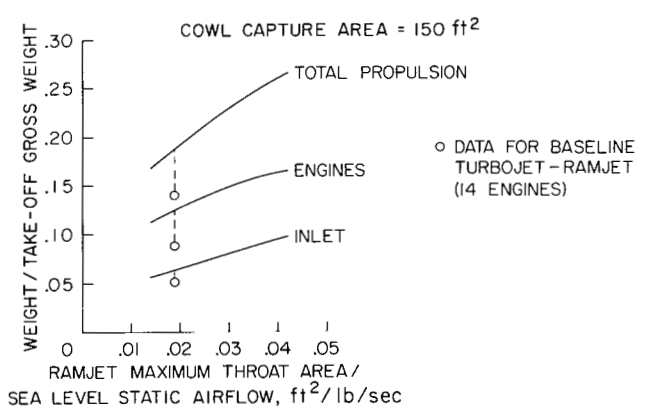

Figure 36.– Propulsion system weights breakdown for the wraparound turboramjet.

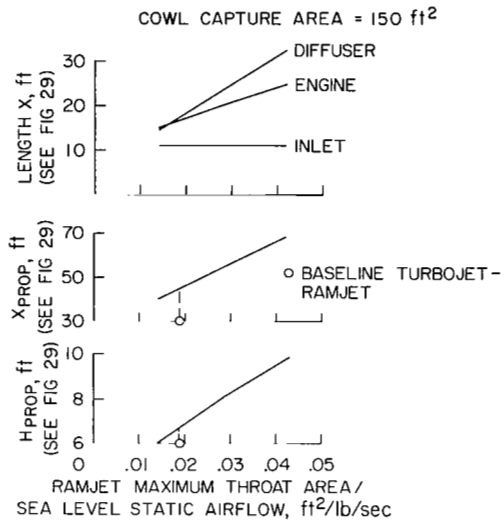

Figure 37.– Installation dimensions for the wraparound turboramjet.

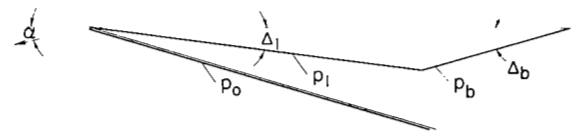

Figure 38.– All-body vehicle lower surface without propulsion package.

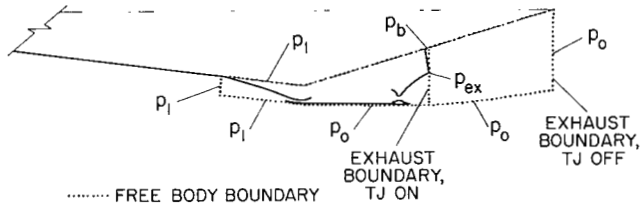

Figure 39.– Propulsion system free-body envelope without spillage.

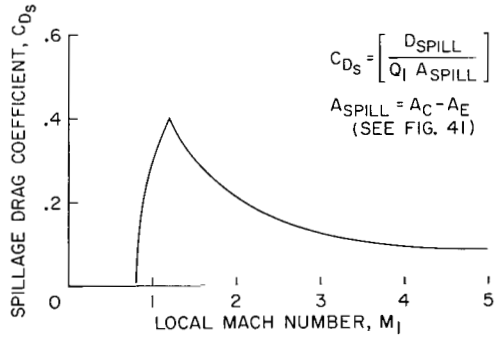

Figure 40.– Spillage drag coefficient.

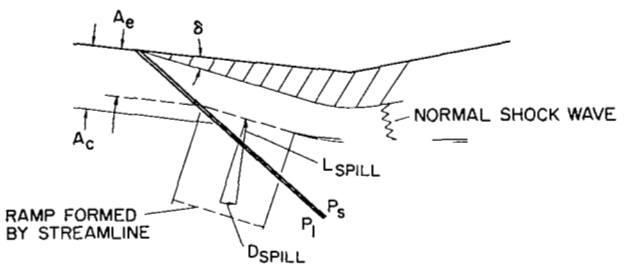

Figure 41.– Additive drag forces for a started inlet.

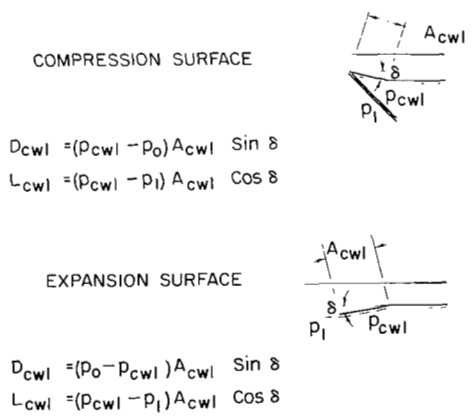

Figure 42.– Cowl forces.

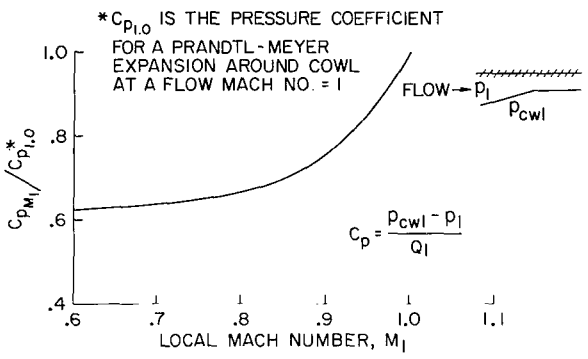

Figure 43.– Cowl pressure coefficient.

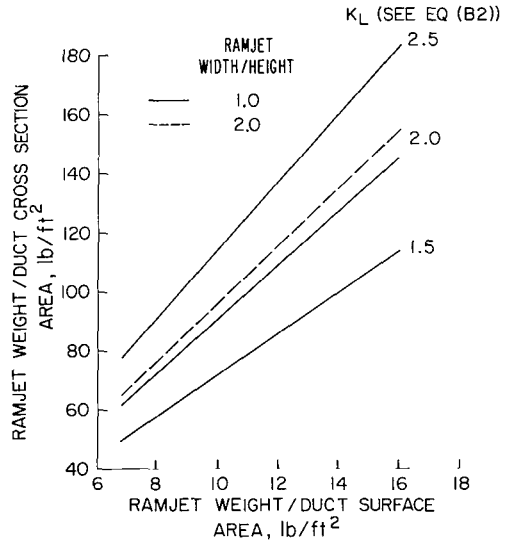

Figure 44.– Ramjet unit weights.

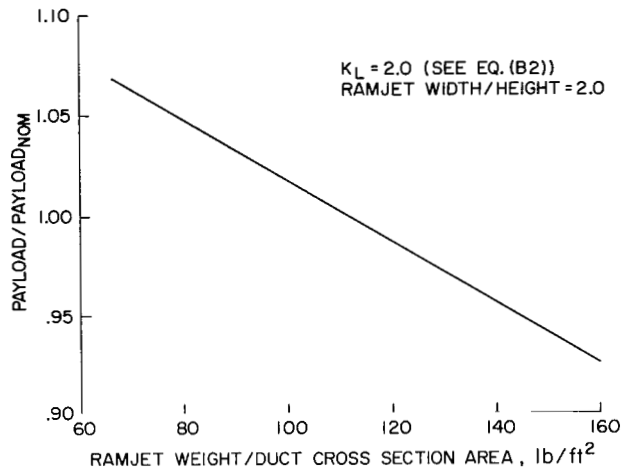

Figure 45.– Effect of ramjet unit weight on vehicle payload.

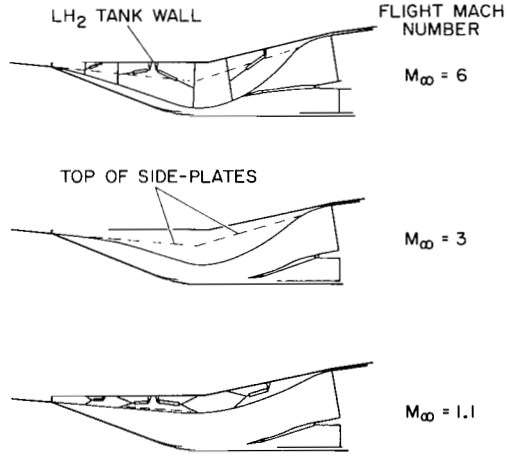

Figure 46.– Inlet configuration for the parallel turbojet-ramjet propulsion system.

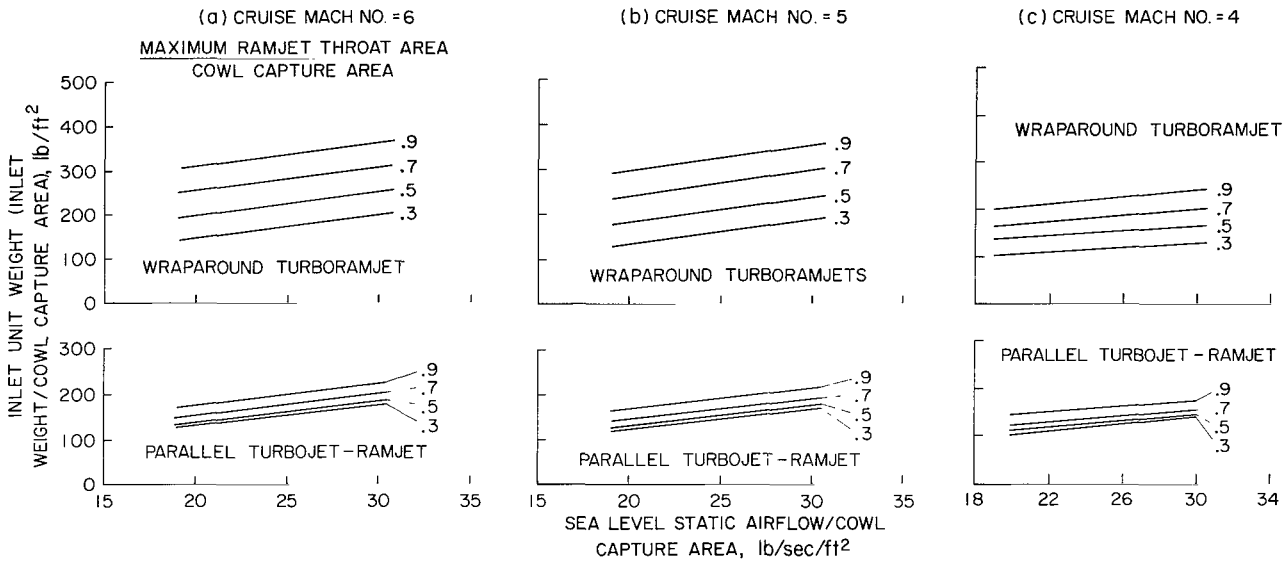

Figure 47.– Two-dimensional inlet unit weights.

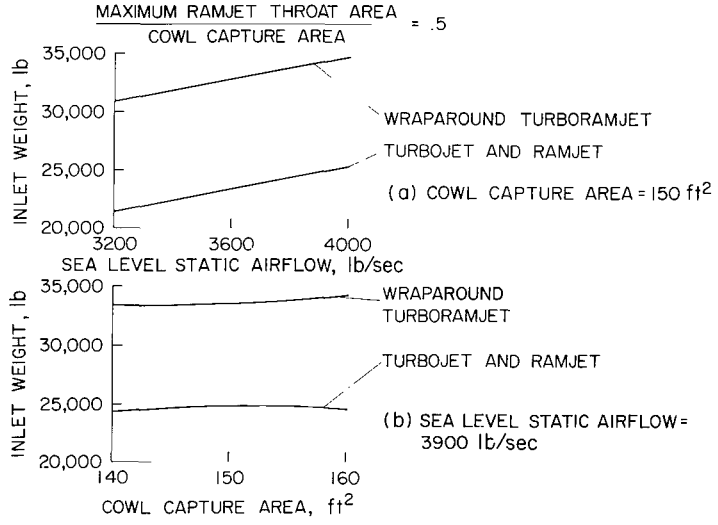

Figure 48.– Inlet weight.

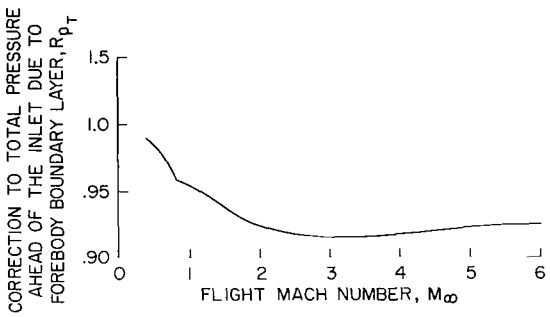

Figure 49. - Boundary-layer correction for total pressure during acceleration to M = 6.

NASA-Langley, 1970 — 28 A-3668

"The aeronautical and space activities of the United States shall be conducted so as to contribute . . . to the expansion of human knowledge of phenomena in the atmosphere and space. The Administration shall provide for the widest practicable and appropriate dissemination of information concerning its activities and the results thereof."

—NATIONAL AERONAUTICS AND SPACE ACT OF 1958

NASA SCIENTIFIC AND TECHNICAL PUBLICATIONS

TECHNICAL REPORTS: Scientific and technical information considered important, complete, and a lasting contribution to existing knowledge.

TECHNICAL NOTES: Information less broad in scope but nevertheless of importance as a contribution to existing knowledge.

TECHNICAL MEMORANDUMS: Information receiving limited distribution because of preliminary data, security classification, or other reasons.

CONTRACTOR REPORTS: Scientific and technical information generated under a NASA contract or grant and considered an important contribution to existing knowledge.

TECHNICAL TRANSLATIONS: Information published in a foreign language considered to merit NASA distribution in English.

SPECIAL PUBLICATIONS: Information derived from or of value to NASA activities. Publications include conference proceedings, monographs, data compilations, handbooks, sourcebooks, and special bibliographies.

TECHNOLOGY UTILIZATION PUBLICATIONS: Information on technology used by NASA that may be of particular interest in commercial and other non-aerospace applications. Publications include Tech Briefs, Technology Utilization Reports and Technology Surveys.

Details on the availability of these publications may be obtained from:

SCIENTIFIC AND TECHNICAL INFORMATION OFFICE

NATIONAL AERONAUTICS AND SPACE ADMINISTRATION

Washington, D.C. 20546